

UC Davis

UC Davis Previously Published Works

Title

Understanding spatial variability of forage production in California grasslands: delineating climate, topography and soil controls

Permalink

<https://escholarship.org/uc/item/8cz960wp>

Journal

Environmental Research Letters, 16(1)

ISSN

1748-9318

Authors

Liu, Han
Jin, Yufang
Roche, Leslie M
et al.

Publication Date

2021

DOI

10.1088/1748-9326/abc64d

Peer reviewed

ACCEPTED MANUSCRIPT • OPEN ACCESS

Understanding spatial variability of forage production in California's grassland: delineating climate, topography and soil controls

To cite this article before publication: Han Liu *et al* 2020 *Environ. Res. Lett.* in press <https://doi.org/10.1088/1748-9326/abc64d>

Manuscript version: Accepted Manuscript

Accepted Manuscript is "the version of the article accepted for publication including all changes made as a result of the peer review process, and which may also include the addition to the article by IOP Publishing of a header, an article ID, a cover sheet and/or an 'Accepted Manuscript' watermark, but excluding any other editing, typesetting or other changes made by IOP Publishing and/or its licensors"

This Accepted Manuscript is © 2020 The Author(s). Published by IOP Publishing Ltd.

As the Version of Record of this article is going to be / has been published on a gold open access basis under a CC BY 3.0 licence, this Accepted Manuscript is available for reuse under a CC BY 3.0 licence immediately.

Everyone is permitted to use all or part of the original content in this article, provided that they adhere to all the terms of the licence <https://creativecommons.org/licenses/by/3.0>

Although reasonable endeavours have been taken to obtain all necessary permissions from third parties to include their copyrighted content within this article, their full citation and copyright line may not be present in this Accepted Manuscript version. Before using any content from this article, please refer to the Version of Record on IOPscience once published for full citation and copyright details, as permissions may be required. All third party content is fully copyright protected and is not published on a gold open access basis under a CC BY licence, unless that is specifically stated in the figure caption in the Version of Record.

View the [article online](#) for updates and enhancements.

Understanding spatial variability of forage production in California's grassland: delineating climate, topography and soil controls

Han Liu^{1*}, Yufang Jin¹, Leslie M. Roche², Anthony T. O'Geen¹, and Randy A. Dahlgren¹

¹Department of Land, Air and Water Resources, University of California, Davis, CA, USA

²Department of Plant Science, University of California, Davis, CA, USA

*Corresponding author: haxliu@ucdavis.edu

Abstract

Rangelands are a key global resource, providing a broad range of ecological services and economic benefits. California's predominantly annual rangelands cover ~40% of the state's land area, and the forage production is highly heterogeneous, making balancing economic (grazing), conservation (habitat) and environmental (erosion/water quality) objectives a big challenge. Herein, we examined how climate and environmental factors regulate annual grassland forage production spatially across the state and among four ecoregions using machine learning models. We estimated annual forage production at a 30-m resolution over a 14-year period (2004-2017) using satellite images and data fusion techniques. Our satellite-based estimation agreed well with independent field measurements, with a R^2 of 0.83 and RMSE of 682 kg/ha. Forage production (14-yr average) showed large spatial variability (2940 ± 934 kg/ha/yr; CV=35%) across the study area. The gradient boosted regression tree with 11 feature variables explained 67% of the variability in forage production across the state. Precipitation amount, especially in November (germination) and April (rapid growth), was found as the dominant driver for spatial variation in forage production, especially in drier ecoregions and during drier years. Seasonal distribution of precipitation and minimum air temperature showed a relatively stronger control on forage production in wetter regions and during wet years. Additionally, solar energy became more important in wetter ecoregions. Drought reduced forage production from the long-term mean, i.e., a $33 \pm 19\%$ decrease in production (2397 ± 926 kg/ha/yr; CV=38%) resulting from a $29 \pm 5\%$ decrease in precipitation. The machine learning based spatial analysis using "big data" provided insights on impacts of climate and environmental factors on forage production variation at various scales. This study demonstrates a cost-effective approach for rapid mapping and assessment of annual forage production with the potential for near real-time application.

Keywords: Ecosystem productivity; Spatial variability; Rangelands; Remote sensing; Data fusion; Gradient boosted regression trees

1. Background

1 Rangelands comprise more than 30% of global land area and provide a broad range of
2 ecosystem services – including food and forage production, soil and water resource
3 protection, biodiversity and wildlife habitat (Parton et al., 2012; Schohr, 2014).
4 California has more than 15 million hectares of annual rangelands, approximately 40%
5 of the state’s land area, ranging from the North Coast to Southern Interior. Nearly 70%
6 of the forage production in California is provided by annual rangelands (UC Rangeland,
7 2017), supporting a \$3.4-billion per year livestock industry (California Department of
8 Food & Agriculture, 2015). However, unlike most perennial systems that can tap deep
9 soil moisture, production of annual grasses/forbs is very sensitive to the water content
10 in the shallow root zone (~30 cm depth), which relies on frequent precipitation for
11 replenishment (Barbour, 2007). As a result, the recent 2012-2016 prolonged drought
12 presented severe challenges to sustainable ranching operations and the ecological
13 services rangelands provide. Most notably, severe drought lead to ecological shifts that
14 significantly impacted forage production (Macon et al., 2016). Due to its diverse
15 climate and topography, California’s forage production varies by as much as fourfold,
16 both interannually at a given location and within a given year at different locations
17 (Becchetti et al., 2016; Larsen et al., 2014). This spatial heterogeneity and temporal
18 dynamics pose challenges for rangeland managers to balance economic (grazing),
19 conservation (habitat) and environmental (erosion/water quality) objectives. Therefore,
20 it is critical to quantify and understand the drivers of spatial/temporal variability in
21 forage production across long- and short-term (e.g., extreme wet/dry) conditions.

22 Growing-season precipitation is generally recognized as the primary driver of annual
23 grassland forage production in the Mediterranean climate of California (Le Houerou,
24 1984). Several studies developed regression equations linking precipitation and/or air
25 temperature with peak annual forage production (Chaplin-Kramer & George, 2013;
26 George et al., 1988, 1989; Murphy, 1970; Pitt & Heady, 1978). While, these studies
27 found positive relationships between peak production and precipitation and air
28 temperature, the relationship was not always simple and displayed considerable site-
29 specific variability. Additionally, an analysis of long-term, peak forage production
30 across California documented above-mean production during years with low but well-
31 distributed precipitation (Becchetti et al., 2016), indicating that temporal variability of
32 precipitation within a given year is also an important factor.

33 At a local scale, topography and soil characteristics affect forage production by
34 regulating solar energy and moisture availability. For example, south versus north
35 slopes have contrasting microclimates that affect the length of the growing season,
36 especially during years with limited rainfall (Hufstader, 1978; Liu et al., 2019). A recent
37 microclimate–forage growth study on a California Central Coast grassland found that
38 wetter topographic locations were more productive in a dry year (water limitation)
39 while warmer topographic locations were more productive in a wet year (energy
40 limitation) (Devine et al., 2019). Soil properties, such as texture, fertility and water
41 holding capacity, also affect vegetation composition and growth characteristics
42 (Bartolome et al., 2007), but are much less studied.

43 Although previous studies examined relationships between forage production and its
44 potential drivers, they were limited in spatial and temporal scale relative to the extent
45 of California rangelands. Satellite remote sensing offers a powerful and cost-effective

1 approach for rangeland monitoring at large spatial and temporal scales (Jones et al.,
2 2018; Reeves et al., 2015). Landsat and MODIS satellites, for example, have collected
3 land observations for resource management at 30-500-m resolution for several decades.
4 Empirical relationships between the Normalized Difference Vegetation Index (NDVI)
5 and green plant photosynthetic activity during the active growing season have been
6 developed and applied to estimate grassland productivity in Europe (Boschetti et al.,
7 2007), Asia (Xu et al., 2008), and America (Gaffney et al., 2018). A vegetation index-
8 based approach was also adopted in a global study to assess the effect of climate change
9 on global grassland productivity from 1982 to 2011 (Gao et al., 2016). More recently,
10 small Unmanned Aerial Systems (sUASs) have been used to estimate finer resolutions
11 of forage production at a catchment scale (Liu et al., 2019). Despite their advantages,
12 satellite remote sensing images are limited by frequent cloud cover during rainy seasons
13 when grasslands are actively growing. For example, considering the 8-16-day Landsat
14 revisit cycle, an overcast day on the overpass date may lead to no useable images for as
15 long as 32 days. However, data fusion techniques make it possible to obtain daily 30-
16 m resolution observations, by combining Landsat with other more frequent but coarser
17 resolution satellite observations such as MODIS (Chen et al., 2015; Gao et al., 2006;
18 Zhu et al., 2010).

19 Previous studies reported that grassland forage production is highly dependent on water
20 availability, which is often a function of a suite of climatic, topographic and edaphic
21 factors (Fuhlendorf et al., 2017). However, most studies of grassland productivity tend
22 to focus on the impact of one set of environmental drivers, either climate, topography
23 or soil properties (Gao et al., 2016; Jin & Goulden, 2014; Willms, 1988), whereas a
24 comprehensive analysis of how these drivers work together to shape production is still
25 lacking. The lack of sufficient field measurements is often an impediment for using
26 traditional statistical approaches. However, recent advances in machine learning
27 methods provide a powerful tool for knowledge discovery from large datasets, by
28 disentangling and visualizing complex relationships (Molnar, 2019).

29 In this study, we mapped grassland forage production at 30-m resolution on California
30 rangelands by fusing Landsat and MODIS satellite data from 2004 to 2017, and
31 investigated how a suite of climate, topography and soil factors determined the spatial
32 variability of the derived 14-yr mean forage production using Gradient boosted
33 regression trees (GBRT) (Friedman, 2001). Specifically, we sought to answer the
34 following questions: (1) What are the main drivers shaping the spatial patterns of forage
35 production of California rangelands? (2) How do these environmental factors affect the
36 production across the state and within each ecoregion? and (3) How do drought versus
37 wet conditions alter these relationships? The results of this study will inform rangeland
38 management and policy decisions and provide insights on productivity of California's
39 diverse rangelands and how their response to future climate change may vary depending
40 on the spatial location within the state.

41 **2. Data & Methods**

42 **2.1 Study Area**

43 This study focused on California rangelands, grasslands in particular, characterized by
44 a Mediterranean climate with hot, dry summers and mild, moderately wet winters

(Becchetti et al., 2016). Our effective study area is $\sim 24,000 \text{ km}^2$, spanning from 33° to 41° N and 118° to 124° W . It represents a mean precipitation gradient of 160 to 2290 mm/yr and elevations from sea level to $\sim 1200 \text{ m}$ (Fig. 1a & b). The area was divided into four ecoregions, based on ECOMAP (Cleland et al., 2007): Northern California Coast Ranges (NCCR), Northern California Interior Coast Ranges (NCICR), Central Coast Ranges (CCR) and Sierra Nevada Foothills (SNF) (See Table S1 for land cover percentages). Precipitation fluctuates widely from year-to-year across the study area with $397 \pm 271 \text{ mm}$ (mean \pm std dev) in the driest year (2014) and $1158 \pm 654 \text{ mm}$ in the wettest year (2017) of the study period. Annual grasses and forbs typically germinate with onset of the rainy season in late fall (November) and reach peak biomass in late spring as the rainy season ceases, typically in April (Larsen et al., 2014). Compositionally, forbs tend to be more prevalent in dry years while grasses are more dominant in wet years (Pitt & Heady, 1978).

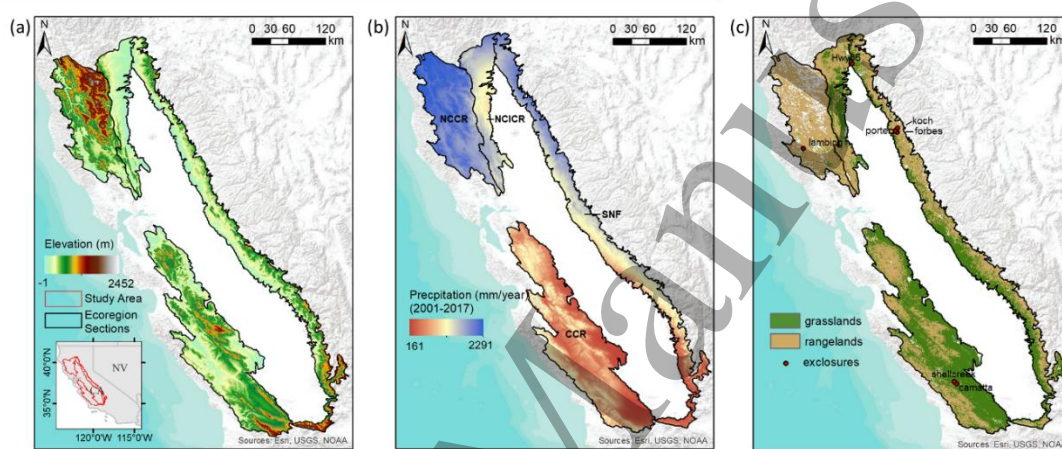


Figure 1. Topography (a) and precipitation (b) of the study area encompassing four ecoregions (MAP (mm/yr): CCR=406, NCICR=674, SNF=681 and NCCR=1278). Only grasslands (c) were included in the study by thresholding on the summer NDVI.

2.2 Data

To calibrate and validate satellite-based forage estimates, we measured monthly dry forage biomass at seven grazing exclosures ($>60 \times 60 \text{ m}$) during two contrasting growing seasons (November to May in 2017 and 2018) (Fig. 1c). Water year 2017 ($>1000 \text{ mm/yr}$) was a wet year while 2018 ($<500 \text{ mm/yr}$) was a relatively drier year. Our sites covered a large environmental gradient, from dry sites in the CCR to northern wetter sites. We clipped 15 to 36, $30 \times 30 \text{ cm}$ quadrats, within each exclosure, depending on exclosure size, and oven-dried the clippings at 60° C for at least 48 hours. Site level biomass measurements were calculated by averaging the quadrat measurements. Sites were mowed or grazed to remove excess dry residual matter at the end of each growing season. In total, we collected 61 site-month measurements across all sites and time (Table S2).

To estimate daily and annual forage production at 30-m across the entire study area, we combined remote sensing observations of surface reflectance in the red and near

1 infrared bands from Landsat and Moderate Resolution Imaging Spectroradiometer
2 (MODIS) satellite instruments for the 2004-2017 period. We downloaded the surface
3 reflectance and the associated quality assessment (PIXELQA) layers of Landsat
4 Analysis Ready Data (ARD, series 5-8) from USGS earth explorer
5 (<https://earthexplorer.usgs.gov/>). Landsat ARD dataset includes Landsat (4-8 series)
6 observations at 30 m acquired from 1982 to present available every 8-16 days. The
7 ARD datasets are geometrically and radiometrically consistent and have flagged non-
8 target features (e.g. clouds and cloud shadows) and poor quality observations, to allow
9 analysis with minimum user preprocessing (Dwyer et al., 2018). At a higher temporal
10 frequency, MODIS sensors have been collecting global multi-spectral images every day
11 at moderate spatial resolutions since 2000. We obtained the MODIS collection 6 daily
12 red and near infrared surface reflectance products at 250 m since 2003 from both Terra
13 (MOD09GA) and Aqua (MYD09GA) instruments from NASA Earthdata
14 (<https://earthdata.nasa.gov/>). Each MODIS product included the corresponding quality
15 assurance (QA) layers.

16 Normalized Difference Vegetation Index (NDVI) (Deering et al., 1975) is a widely used
17 proxy for photosynthetic activity and primary production (Carlson & Ripley, 1997). We
18 calculated NDVI from both Landsat and MODIS surface reflectance. Initial filtering
19 removed low quality observations, i.e. those affected by clouds and cloud shadows,
20 based on the corresponding QA layers. Invalid pixels in MODIS images were
21 interpolated from temporally neighborhood images using a cubic interpolation method.

22 We used Daymet climate data from the Oak Ridge National Laboratory Distributed
23 Active Archive Center (ORNL DAAC) to assess drivers of spatial variation in forage
24 production. The gridded daily surface weather parameters at a 1-km spatial resolution
25 were interpolated from more than 8,000 meteorological stations, based on a digital
26 elevation model (Thornton et al., 2016). We downloaded Daymet climate data during
27 the same time period as the MODIS data (2004-2017). Compared to a longer historical
28 time period (1986-2017), annual precipitation during 2004-2017 was 18 mm/yr lower
29 and mean air temperature was 0.2 °C higher. We aggregated daily precipitation,
30 min/max/mean air temperatures, and solar radiation to monthly averages. Seasonal
31 averages that were potentially related to forage production were further derived as
32 detailed in Table 1. We calculated the Precipitation Concentration Index (PCI) (Oliver,
33 1980) to depict precipitation variation between the driest and wettest month during the
34 growing season (November to May) (Sloat et al., 2018) and growing degree days using
35 a baseline temperature of 4°C. We chose to use 4°C as the baseline temperature because
36 young annual plants in California grow very slowly at temperatures between 4.4 –
37 10.5°C (Becchetti et al., 2016). For spatial analysis, we derived long-term means for 29
38 variables from water year (Oct-Sept) 2004 to 2017 (Table 1).

39 Shuttle Radar Topography Mission (SRTM) 1 Arc-second (30-m) global elevation data
40 were used for topographic characterization. We derived aspect, slope and water flow
41 direction (flow accumulation and curvature) using ArcMap 10.6.1. We also calculated
42 illumination condition (IC), a widely used measure for topography-modulated lighting
43 conditions: -1 (less light) to +1 (more light) (Tan et al., 2013).

44 Grasslands mostly exist in well-drained areas below 1200-m elevation and occur on

1 diverse soil types (Jackson & Bartolome, 2007). We obtained the 800-m resolution
 2 aggregated and rasterized SSURGO soil property dataset from California Soil Resource
 3 Lab (<https://soilmap2-1.lawr.ucdavis.edu/mike/soilweb/soil-properties/download.php>).
 4 Rasterized SSURGO datasets were derived based on thickness-weighted average
 5 values to aggregate horizons within soil profiles and spatially-weighted averages of
 6 map units within grids (Beaudette et al., 2013; O'Geen et al., 2017). Selected soil
 7 properties for the 0-25 cm layer (dominant rooting zone for grasses/forbs) that were
 8 expected to most strongly affect forage production were downloaded: clay, sand, silt,
 9 water holding capacity, bulk density and soil organic matter. The Daymet climate data
 10 and rasterized SSURGO data sets, originally at 1000- and 800-m spatial resolution,
 11 were resampled to 30 m using a cubic resampling method to match satellite and
 12 topographic data grids.

13 2.3 Forage production estimation with satellite data fusion

14 We estimated forage production as a function of absorbed photosynthetically active
 15 radiation (APAR) accumulated during the growing season (cAPAR) (Eq. 1, Fig. 2).

$$16 \quad LUE \times \text{sum}(APAR) = LUE \times \text{sum}(PAR \times fPAR) \dots \dots (1)$$

17 PAR was estimated from daily shortwave incoming solar radiation at 2-km resolution
 18 (Hart et al., 2009), assuming a constant ratio of 0.5 (Akitsu et al., 2015; Blackburn &
 19 Proctor, 1983; Li et al., 2010; Papaioannou et al., 1993). The CIMIS program generates
 20 all sky shortwave incoming solar radiation for California, based on GOES satellite
 21 observations (Hay, 1993).

22 We followed an approach introduced by Sellers et al. (1996) to calculate fPAR as a
 23 function of NDVI and simple ratio (SR) of NIR reflectance over red reflectance:

$$24 \quad fPAR = 0.5 * (fPAR_{NDVI} + fPAR_{SR}) \dots \dots (2)$$

$$25 \quad fPAR_{NDVI} = \frac{(NDVI - NDVI_{min})(fPAR_{max} - fPAR_{min})}{NDVI_{max} - NDVI_{min}} + fPAR_{min} \dots \dots (3)$$

$$26 \quad fPAR_{SR} = \frac{(SR - SR_{min})(fPAR_{max} - fPAR_{min})}{SR_{max} - SR_{min}} + fPAR_{min} \dots \dots (4)$$

27 where the minimum and maximum fPAR ($fPAR_{min} = 0.001$, $fPAR_{max} = 0.95$)
 28 correspond to the lower and upper 2% of the NDVI histogram ($NDVI_{min}$ and $NDVI_{max}$).
 29 $NDVI_{min}$ and $NDVI_{max}$ were set to 0.015 and 0.760, respectively, based on values
 30 derived in Los et al. (2000). We applied the same procedure for SR_{min} and SR_{max}
 31 generating values of 1.030 and 7.333, respectively.

32 California rangelands grow rapidly during the rainy season, when clear sky satellite
 33 imagery is sometimes limited, especially for Landsat with a 16-day revisiting interval.
 34 We, therefore, implemented a Spatial and Temporal Adaptive Reflectance Fusion
 35

1 Model (STARFM) (Gao et al., 2006; Liu et al., 2019) to fully exploit the
2 complementary resolutions of Landsat and MODIS data. The STARFM approach
3 combines the spatial resolution of Landsat (30 m) with the temporal resolution of
4 MODIS (daily at 250 m). The approach uses one or more pairs of concurrent Landsat
5 and MODIS images to predict Landsat resolution images on days when Landsat data
6 were unavailable. We used a 48-day time window when searching for image pairs,
7 prioritizing dates with clean pixels and dates that were closer to the date of prediction.
8 This fusion approach generated continuous daily NDVI images at 30-m resolution (Fig.
9 S1a-c). We applied an enhanced Savitzky–Golay filter (Chen et al., 2004) to the fused
10 NDVI time series to remove abnormal values. The filtered time series followed similar
11 temporal patterns with those from MODIS data while keeping the spatial details from
12 Landsat observations (Fig. S1d). To mask trees and other perennial vegetation, we only
13 kept pixels where NDVI was smaller than 0.3 in mid-August (Fig. 1c), because annual
14 herbaceous plants are senescent in August.

15 The beginning and end of each growing season was estimated by fitting two sigmoidal
16 curves stitching the fused daily NDVI time series (Zhang et al., 2003) (See appendix).
17 The green-up and senescence dates were defined as the dates with the largest
18 increase/decrease of NDVI based on the curvature of the simulated curves (Fig. S2).
19 We then estimated the annual cumulative APAR (cAPAR) as the sum of daily APAR
20 over the identified growing seasons for each 30-m pixel and for each year during 2004-
21 2017 (Fig. 2). We found a strong linear relationship between cAPAR and measured
22 monthly dry biomass for all seven exclosures ($R^2=0.83$) (Fig. 3a). A linear regression
23 was developed to relate forage production with cAPAR, using 70% of the data for
24 training and the remaining 30% for testing. The slope showed an average light use
25 efficiency (LUE) of 0.55 g/MJ APAR. The estimated forage production explained 83%
26 of variation with a RMSE of 681 kg/ha, when validated using the testing dataset (Fig.
27 3b&c).

28 We estimated annual forage production from the calibrated LUE over each 30-m pixel
29 for the 14 growing seasons in this study (2004-2017). Long-term mean (LTM) forage
30 production was generated for the entire 14-yr record, drought years (water years 2007-
31 09 and 2012-15) (Asner et al., 2016; Ghosh, 2019; Williams et al., 2015) and extremely
32 wet years (water years 2005, 2006 and 2017) with >1000 mm/yr annual precipitation.
33 We quantified the relative departure from the long-term production during the extreme
34 dry and wet periods (departure normalized by LTM). It is important to note that
35 California grasslands are predominantly a grazed landscape. Since our forage
36 estimation is based on daily cumulative APAR throughout the active growing season,
37 “forage production” carries different meanings in grazed vs. ungrazed areas. In
38 ungrazed areas, forage production is equivalent to the peak forage production, whereas
39 in grazed areas, it is the sum of standing crop and livestock consumption.

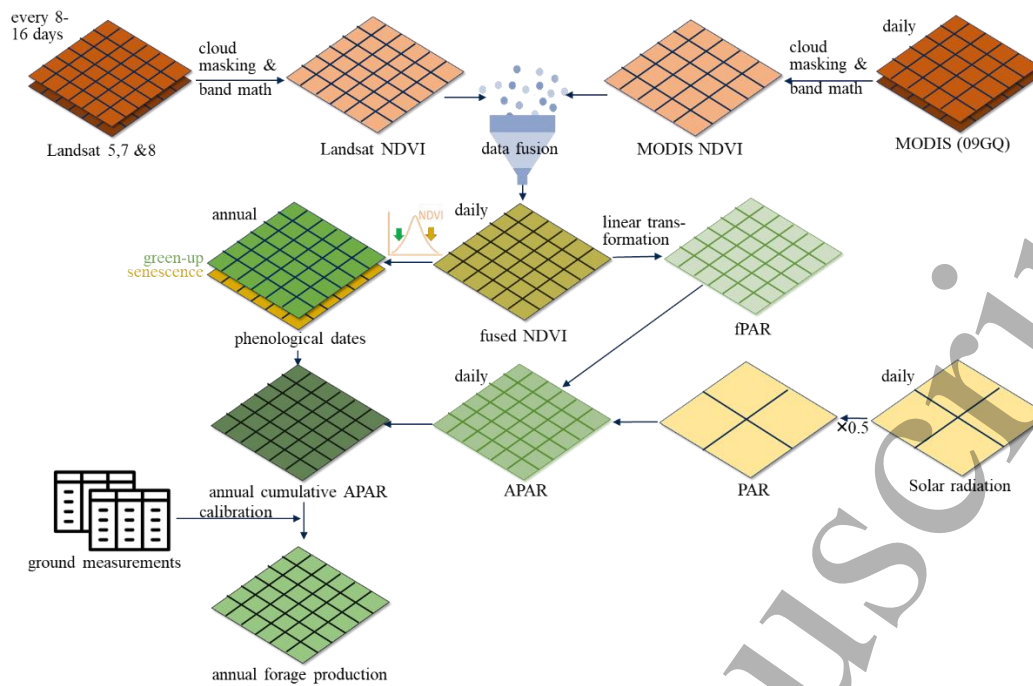


Figure 2. Flowchart for forage production estimation with data fusion. We first generated daily NDVI images at 30-m resolution by fusing Landsat and MODIS data. The fused NDVI was then converted to fPAR. We estimated forage production as a function of absorbed photosynthetically active radiation (APAR) accumulated during the growing season (cAPAR).

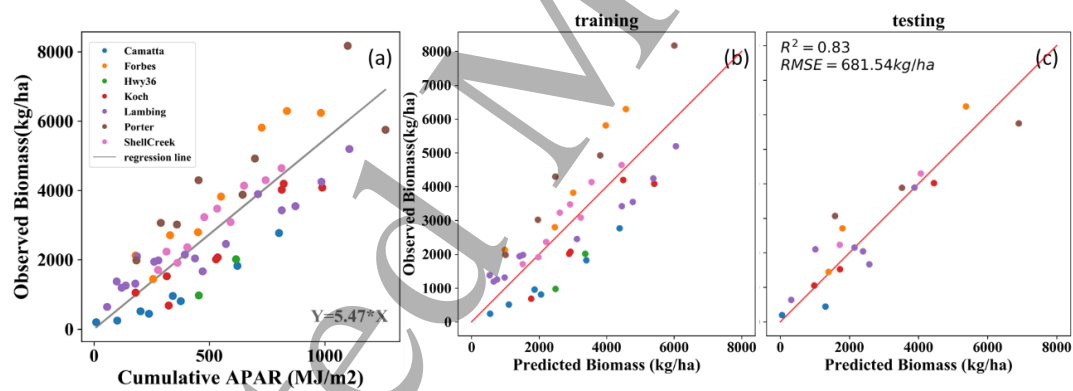


Figure 3. Scatterplots of cumulative APAR from satellite versus forage production measurements over seven field sites (color coded) show a strong linear relationship ($n=61$) (a). Regression based on 70% of the randomly selected data (b) resulted in a R^2 of 0.83 and a RMSE of 682 kg/ha when validated using the other 30% of the data (c) ($n=19$).

2.4 Gradient boosted regression trees and feature selection

To understand the complex relationships between forage production and potential environmental drivers, we used the Gradient boosted regression trees (GBRT) machine learning model (Friedman, 2001) available at the “scikit-learn” library in Python (Pedregosa et al., 2011). GBRT fits regression trees sequentially, with each tree aimed

at minimizing the prediction residuals of its predecessors. To reduce correlations between trees, it uses a random subsample of the training data for fitting each tree, and only considers a portion of the input features at a time for each node. The final prediction is the sum of all regression trees multiplied by a learning rate (lr).

We randomly sampled 10% of the pixels ($n=2,600,000$, Fig. S3) in our study area, which were further randomly split (70 vs. 30%) for model training and testing. We tuned the model hyperparameter by grid search, and set $n=100$, $subsample = 0.6$, $max_depth = 6$, $max_features = 1.0$, $lr = 0.1$ (see SI – Section 1). We started with 41 independent variables and found a large degree of inherent autocorrelation (Fig. S4). Therefore, we grouped these variables into 11 features based on correlations, i.e. variables with $r>0.7$ were grouped (Table 1). Hereafter, “feature” refers to the 11 independent variable sets, and “variable” refers to the 41-individual climatic, topographic and soil metrics (see SI – Section 2 for more information).

We built ensemble models, by allowing only one variable in each feature group to be included in a GBRT model each time to reduce autocorrelation between variables. We first built a baseline model using the first variable within each feature as listed in Table 1, and then another ten models were built by replacing the “GS_ppt” variable with the other 10 variables in feature group 1, one at a time. Finally, we looped through all feature groups that had more than one variable and built 30 additional models.

Table 1. List of variables and feature groups used as predictors for the forage production models. Seasonal variables include averages during growing season (GS, November-June), early, mid- and late seasons (November-January, January-March, March/April-June), winter refers to December to February, which was further split into early and late winter (November-January and January-March).

Group	Feature type (unit)	Variable names and abbreviations	Data source/reference
1 (n=11)	Precipitation amount (mm)	Seasonal: GS_ppt, EarlyS_ppt, MidS_ppt, LateSApr_ppt, LateSMar_ppt Monthly: M11_ppt, M12_ppt, M01_ppt, M02_ppt, M03_ppt, M04_ppt,	Daymet (Thornton et al., 2016)
2 (n=1)	Precipitation distribution	Precipitation concentration index (PCI)	Daymet (Thornton et al., 2016; Oliver, 1980)
3 (n=6)	Minimum air temperature (°C)	GS_tmin, M11_tmin, M12_tmin, M01_tmin, M02_tmin, M03_tmin	Daymet (Thornton et al., 2016)
4 (n=9)	Mean air temperature ¹ (°C)	GS_tave, M11_tave, M12_tave, M01_tave, M02_tave, M03_tave, Winter_tave, WinterEarly_tave, WinterLate_tave	Daymet (Thornton et al., 2016)
5 (n=2)	Incoming solar radiation and maximum Temperature	GS_srad (W/m ²), GS_tmax (°C),	Daymet (Thornton et al., 2016)
6 (n=1)	Elevation (m)	Elevation	SRTM (Rabus et al., 2003)

7 (n=2)	Insolation	Aspect ² , Illumination condition, IC	SRTM(Rabus et al., 2003/Tan et al., 2013)
8 (n=1)	Slope (degree)	Slope	SRTM (Rabus et al., 2003)
9 (n=1)	Curvature	Curvature	SRTM (Rabus et al., 2003; Zevenbergen & Thorne, 1987)
10 (n=1)	Flow accumulation	Flowaccumulation	SRTM (Rabus et al., 2003; Jenson & Domingue, 1988)
11 (n=6)	Soil properties	Water holding capacity (whc - cm), Clay, Sand & Silt (%), Bulk density (bd - g/cm ³), Soil organic matter (som - kg/m ³)	Rasterized SSURGO (Beaudette et al., 2013; O'Geen et al., 2017)

¹Growing degree day variables were removed due to high correlation with mean air temperature. ²Aspect was converted to a continuous variable by $\cos(\text{aspect})$ where -1 represents south and $+1$ represents north.

2.5 Determinants of spatial variation in forage production

We examined the relative contribution of each predictor to spatial patterns of forage production using feature importance, quantified by the mean decrease in the impurity by each input variable based on the GBRT models (Breiman et al., 1984). Impurity represents how poorly the observations at a given node fit the model, measured by the residual sum of squares within that node in a regression tree. For reduced models, we averaged feature importance by feature group and calculated the standard deviation within each group.

Additionally, we used partial dependence plots (PDPs) to quantify how forage production varies spatially with each independent variable. Partial dependence marginalizes the machine learning model over the distribution of other independent variables, so that the remaining function shows the relationship between the targeting variable and dependent variable (Molnar, 2019). The y-axis of PDPs represents the difference between the marginalized prediction and the mean prediction. For example, a wide range on the y-axis indicates a strong sensitivity of forage production to the target predictor, suggesting a strong controlling effect with confounding factors excluded. A partial dependence curve with positive slope suggests a positive relationship and vice versa.

3. Results

We first report the overall spatial patterns of forage production (3.1) and performance of the GBRT models in capturing the spatial variability (3.2). The determinants of spatial variation in long-term mean production are presented in Section 3.3. Section 3.4 further examined drought vs. wet year production. Within each section, we report results for the whole study area first, followed by results for each ecoregion.

3.1 Spatial patterns in long-term forage production

Estimated mean annual forage production (2940 ± 934 kg/ha/yr) from satellite observations over the 2004-2017 study period showed large spatial variability, with a

CV of 35% across the study area (Fig. 4a). The Central Coast Ranges (CCR) had much lower production (2610 ± 890 kg/ha, Table 2), where the driest areas of the ecoregion with precipitation less than 200 mm/yr (Fig. 1b) had a mean annual production of less than 2000 kg/ha (Fig. S5). In contrast, 11% of the study area had very high forage production (>4000 kg/ha/yr), including the northern tip of CCR, central Sierra Nevada Foothills (SNF), a large portion of North California Coast Ranges (NCCR) and several valleys in North California Interior Coast Ranges (NCICR). We found similar spatial patterns for production averaged over dry and wet years (Figs. 4b&c). However, drought-year production (2397 ± 926 kg/ha/yr; CV=38%) was lower and had a higher spatial variability than wet-year production (3722 ± 1080 kg/ha/yr; CV=29%).

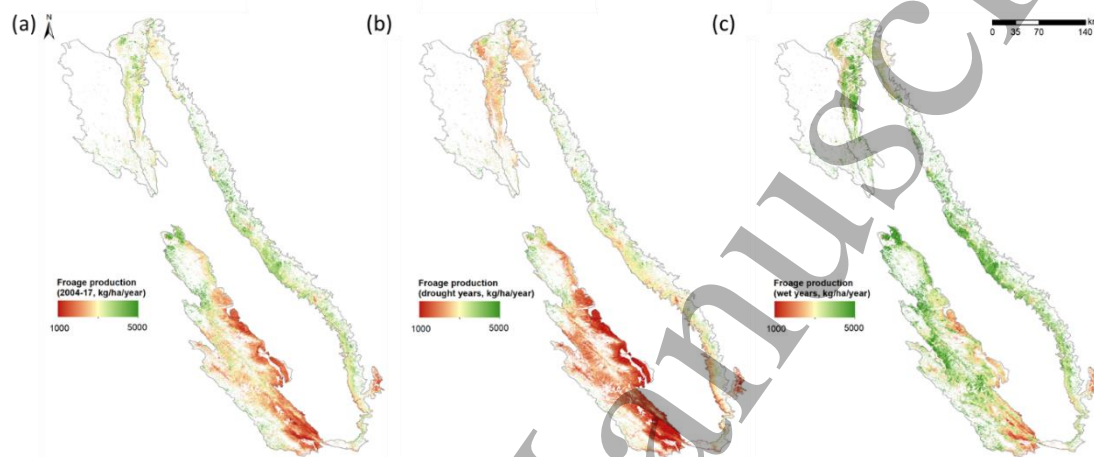


Figure 4. Spatial distribution of cAPAR-derived mean forage production averaged over (a) 2004-17, (b) drought years, and (c) wet years.

3.2 GBRT model performance

The GBRT model effectively captured the spatial variability of satellite-based LTM forage production at 30-m resolution across the entire study area. Predicted forage production was in good agreement with the estimated forage production in the randomly selected testing data ($R^2=0.70$ and $RMSE=507$ kg/ha), when using all 41 variables as input (Table 2, full model). Reduced models with 11 predictors, one variable from each of the 11 feature groups, had slightly reduced performance with a $RMSE=535 \pm 4$ kg/ha, explaining 67% ($\pm 0.5\%$) of spatial variability (Table 2; Table S3). The predicted forage production map (Fig. 5) showed very similar spatial patterns as those from the satellite-based estimates, even though the model was trained with 10% of the pixels (Fig. 4a). More than 84% of the area had an absolute percent error between modeled vs. satellite estimates lower than 20% (Fig. S6) and the mean absolute percent error was 11.8% averaged over the study area. Among ecoregions, the CCR ecoregion showed the highest prediction accuracy (Table 2).

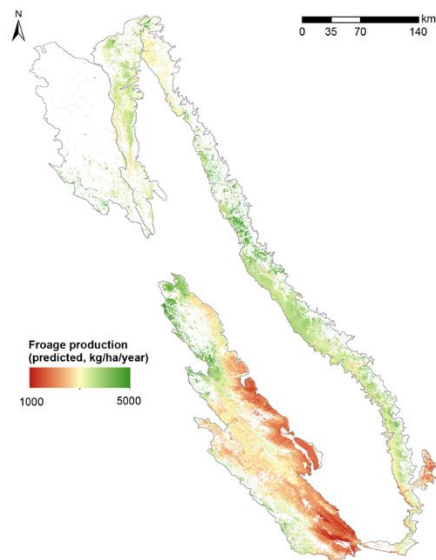
Models built specifically for mean production during drought years performed better than the LTM models ($R^2=0.74 \pm 0.004$ and $RMSE=425 \pm 4$ kg/ha) (Table 2). In contrast, wet-year production models displayed larger uncertainty in capturing the spatial variability ($R^2=0.52 \pm 0.009$ and $RMSE=675 \pm 6$ kg/ha). However, the mean and absolute

percentage errors were similar for drought vs. wet years (Table 2).

Table 2. Model evaluation based on the independent testing data. GBRT models were built for the entire study area and specific ecoregions during the 2004-2017 study period, as well as wet (water years 2005, 2006 and 2017) vs. dry (water years 2007-09 and 2012-15) years.

Region (N*)	Time span	Forage production ** (kg/ha/yr)	Precip. (mm/yr)	Min air temp (°C)	R ²	RMSE (kg/ha/yr)	Mean % error	Abs. % error
<i>Full model (with 41 variables)</i>								
Entire study area (~2.6 M)	All years	2940 ±934	712 ±396	3.8 ±1.3	0.70	507	2%	12%
<i>Reduced models (with 11 variables/features)</i>								
Entire study area (~2.6 M)	All years	2940 ±934	712 ±396	3.8 ±1.3	0.67	536±4	2%	17%
Entire study area (~2.6 M)	Drought years	2397 ±911	519 ±317	3.8 ±1.3	0.74	425±4	1%	18%
Entire study area (~2.6 M)	Wet years	3675 ±1076	1053 ±539	4.0 ±1.4	0.52	675±6	1%	18%
Northern California Coastal Ranges (NCCR, 14K)	All years	3718 ±1230	1274 ±294	2.9 ±1.4	0.61	771	3%	19%
Sierra Nevada Foothills (SNF, ~3M)	All years	3430 ±794	674 ±282	3.8 ±1.5	0.60	504	2%	11%
Northern California Interior Coastal Ranges (NCICR, ~1M)	All years	3332 ±610	753 ±185	4.5 ±0.7	0.43	460	2%	11%
Central Coastal Ranges (CCR, ~1M)	All years	2610 ±890	404 ±109	4.2 ±1.0	0.71	482	3%	14%

*N represents the number of pixels for the domain. **Standard deviations associated with the reduced study area models were calculated from the ensemble models. R² and RMSE were based on comparison with the corresponding independent test datasets. Mean percent error is the average of percent errors over all pixels, where percent error is actual error divided by the remote sensing estimation. Relative difference (absolute percent-errors) were calculated as the mean absolute percent error over all pixels, i.e., dividing the absolute difference between the GBRT predicted and remote sensing estimated forage production by remote sensing estimation.



1
2
3
4
5
6
7
8
9
10
11
12
13
14
15
16
17
18
19
20
21
22 Figure 5. Gradient boosted regression tree estimated long-term mean forage production
23 map.

24 3.3 Determinants of spatial variation in forage production

25
26
27 Over the entire study area, total amount and monthly distribution of precipitation were
28 the two most influential variables controlling the spatial variation in long-term forage
29 production (Fig. 6). Together, these two features reduced more than 40% of impurity
30 across all splits within each regression tree. Partial dependence plots (PDPs) showed
31 that forage production increased rapidly with an increase in growing season
32 precipitation before reaching a plateau at ~450 mm/yr (Fig. 7a). PDP distributions were
33 skewed toward negative values, indicating that low precipitation amount has a stronger
34 negative impact on forage production than a corresponding positive impact from high
35 precipitation. For example, in the more arid regions, forage production was enhanced
36 by 1000 kg/ha when precipitation increased from 300 to 450 mm/yr.
37
38
39

40 November precipitation, in particular, had the strongest impact on forage variability
41 (Fig. S7), with a ~1750 kg/ha difference in forage production when precipitation varied
42 from the driest (15 mm) to the wettest regions (90 mm, Fig. S8a). In contrast, January
43 precipitation had the weakest impact, with an 850 kg/ha difference in forage production
44 across the driest (50 mm) to wettest regions (140 mm). Notably, April precipitation (Fig.
45 S8b) showed the strongest per-unit precipitation influence on forage production. Every
46 1-mm increase in April precipitation resulted in an average 29 kg/ha increase in annual
47 forage production.
48
49

50
51 Areas with more evenly distributed precipitation (i.e., lower PCI, concentrated in the
52 SNF and NCICR, Fig. S9) had higher forage production than those with less evenly
53 distributed precipitation (i.e., higher PCI, spreading across the southwestern CCR, Fig.
54 S9), given the same amount of precipitation (Fig. 7b). The impact from precipitation
55 distribution was more pronounced when PCI varied from 12 to 13.5 than at higher
56 values. The difference in forage production was approximately 500 kg/ha between
57 locations with the lowest and highest PCI values.
58
59

30
60 Minimum temperature was the third most influential feature in regulating the spatial

1 variation of forage production (Fig. 6a). For example, a warmer minimum temperature
2 during the growing season increased the production by 200 kg/ha beyond 4.3°C (Fig.
3 7c). We observed slightly higher forage production in colder areas (<3 °C), mostly at
4 higher elevations in the NCCR region where precipitation is high (Fig. 7c; Fig. S10a).

5 Elevation, mean air temperature and solar energy had intermediate impacts on forage
6 production (~10% importance). Forage production steadily decreased as elevation
7 increased from 150 to 900 m (Fig. 7d). Compared to the mean for the entire study area,
8 forage production at 900 m elevation was 150 kg/ha lower but 100 kg/ha higher at 150
9 m elevation. When everything else was held at their mean values, areas with cooler
10 growing season mean air temperature were more productive than warmer areas (Fig.
11 7e). The relationship between solar radiation and forage production showed an
12 asymmetrical bell shape (Fig. 7f), peaking at 250 W/m² (Fig. S10b). However, the
13 lowering effect was more pronounced at higher values of solar radiation.

14 The next most important feature was soil properties (Fig. 6a). Higher plant available
15 water holding capacity enhanced forage production (Fig. 7g). As the 0-25-cm available
16 water holding capacity increased from 2.5 to 4.5 cm, forage production increased from
17 100 kg/ha below to 75 kg/ha above the overall mean forage production, when all other
18 predictors were held at their mean values. Slope contributed another ~5% of importance
19 with steep slopes generally less productive (e.g., 300 kg/ha lower on a 25° slope) than
20 those on flat areas (Fig. 7h). Variables related to insolation affected forage production
21 slightly. For example, south-facing areas were generally less productive than north-
22 facing areas with an average difference of 140 kg/ha (Fig. 7i). Curvature and flow
23 accumulation had very limited impact on forage production at the statewide level (Fig.
24 6).

25 At the sub-regional scale, the ecoregion-specific models showed different dominant
26 controls for spatial variation in LTM forage production (Fig. 8). Overall, precipitation
27 amount played a more important and dominant role in drier ecoregions (CCR & SNF,
28 Table S4), whereas energy and temperature became more important in wetter
29 ecoregions (NCCR & NCICR). In the wettest region (NCCR), for example, minimum
30 air temperature (see PDP in Fig. S11) was the most important (15%), while all other
31 non-topography related features plus elevation had a similar contribution (10%) (Fig.
32 8c). Similarly, in the NCICR ecoregion (second wettest ecoregion), forage production
33 variation was a mixed effect of climate, solar energy, elevation and soil properties,
34 although precipitation amount became the most influential feature (Fig. 8d).

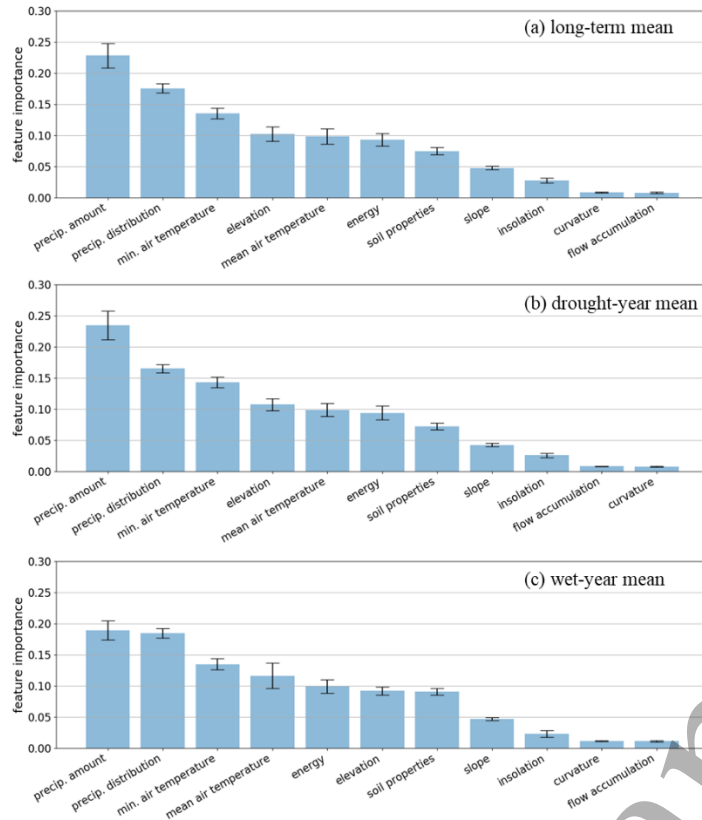
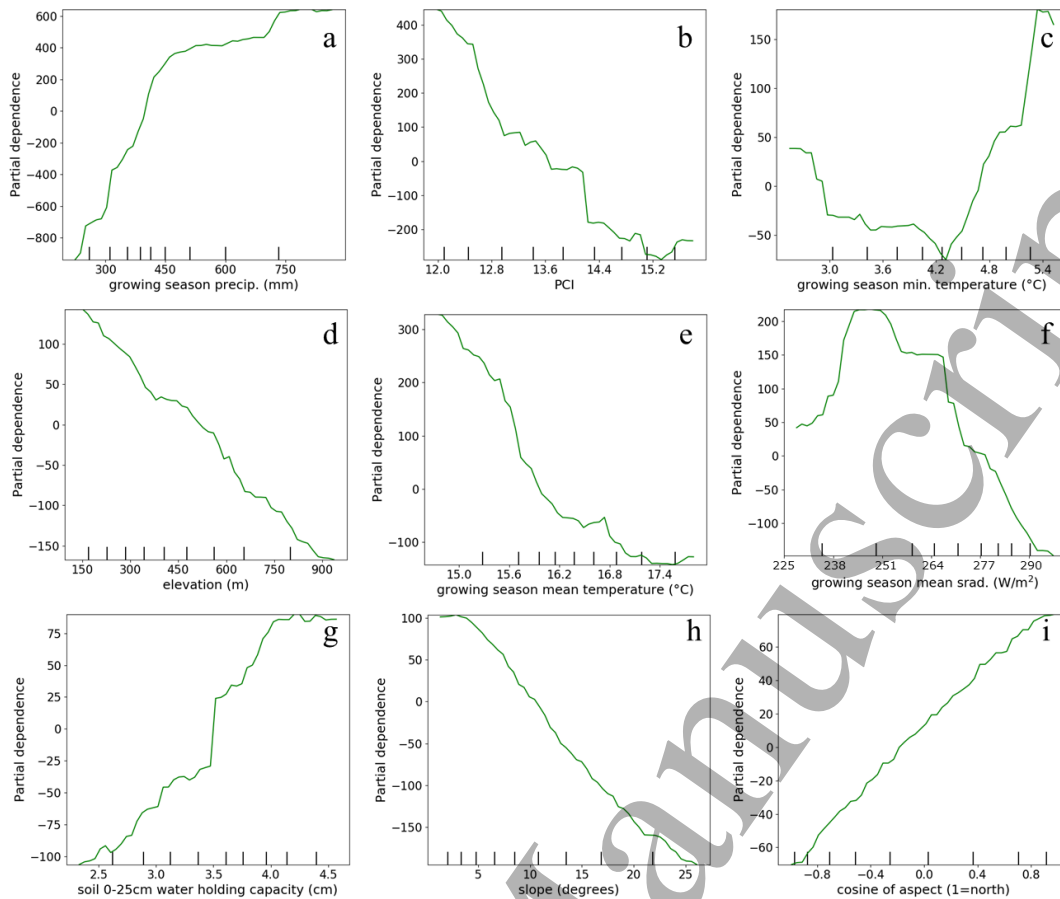
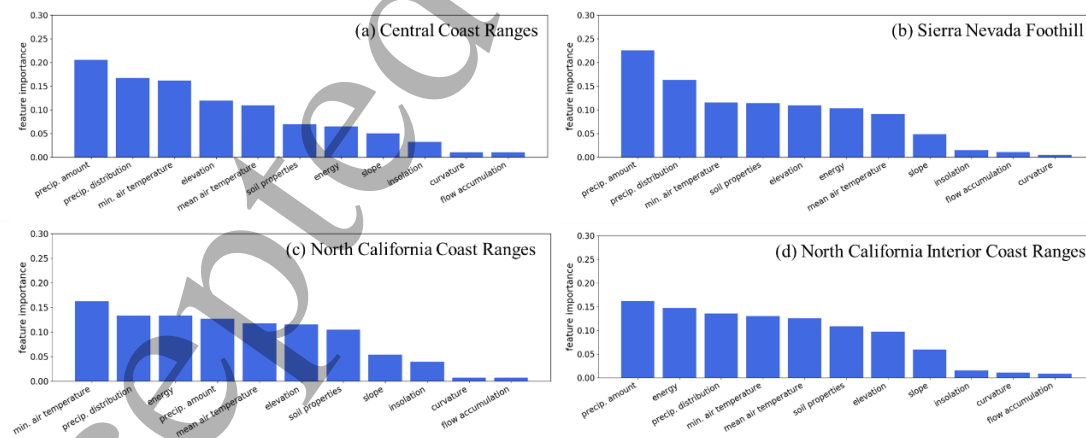


Figure 6. Feature importance of reduced models for different time periods: (a) 2004-17; (b) drought years; (c) wet years. Relative importance of precipitation amount differed under different water availability conditions.



1

2 Figure 7. Partial dependence of long-term mean forage production on (a) growing
 3 season total precipitation, (b) precipitation concentration index (PCI), (c) growing
 4 season minimum temperature, (d) elevation, (e) growing season mean temperature, (f)
 5 growing season mean solar radiation, (g) soil water holding capacity at 0-25 cm, (h)
 6 slope, and (i) cosine of aspect. Marks on the x-axis indicate the data distribution.



7

8 Figure 8. Feature importance of reduced models for the four ecoregions. Drier regions
 9 are more influenced by precipitation amount while wetter regions receive a stronger
 10 influence from other factors.

11

3.4 Forage production under drought versus wet conditions

Drought reduced forage production relative to the LTM, but not by the same magnitude across the state. For example, production was reduced by 612 ± 315 kg/ha/yr ($23 \pm 12\%$) across the study area, when the precipitation decreased from the LTM by 140 ± 46 mm/yr ($31 \pm 5\%$) during drought years (Fig. 9a). Larger departures occurred in less productive areas, such as a decrease by more than 40% on the west side of the Central Coast and $\sim 20\%$ in lower foothills in dry years (Fig. 9a). During wet years, similar patterns were found for increased production, but with a higher departure, i.e., 882 ± 521 kg/ha/yr ($33 \pm 20\%$) due to a MAP increase of 245 ± 89 mm/yr ($56 \pm 12\%$) (Fig. 10b).

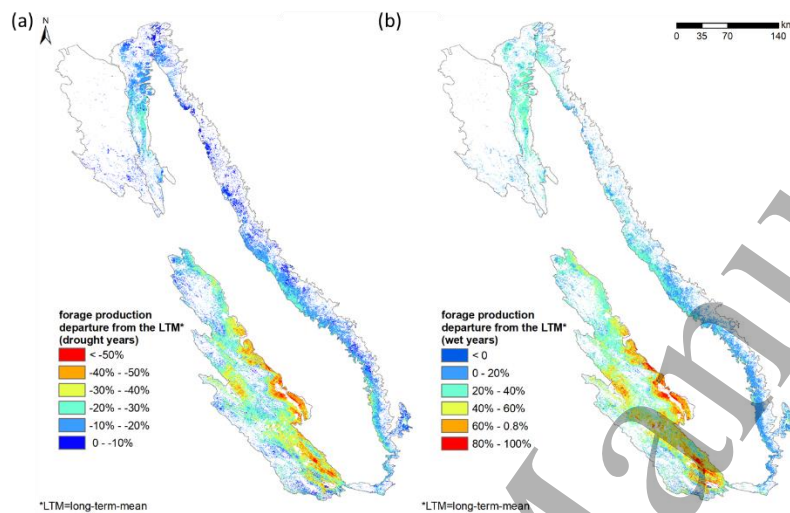


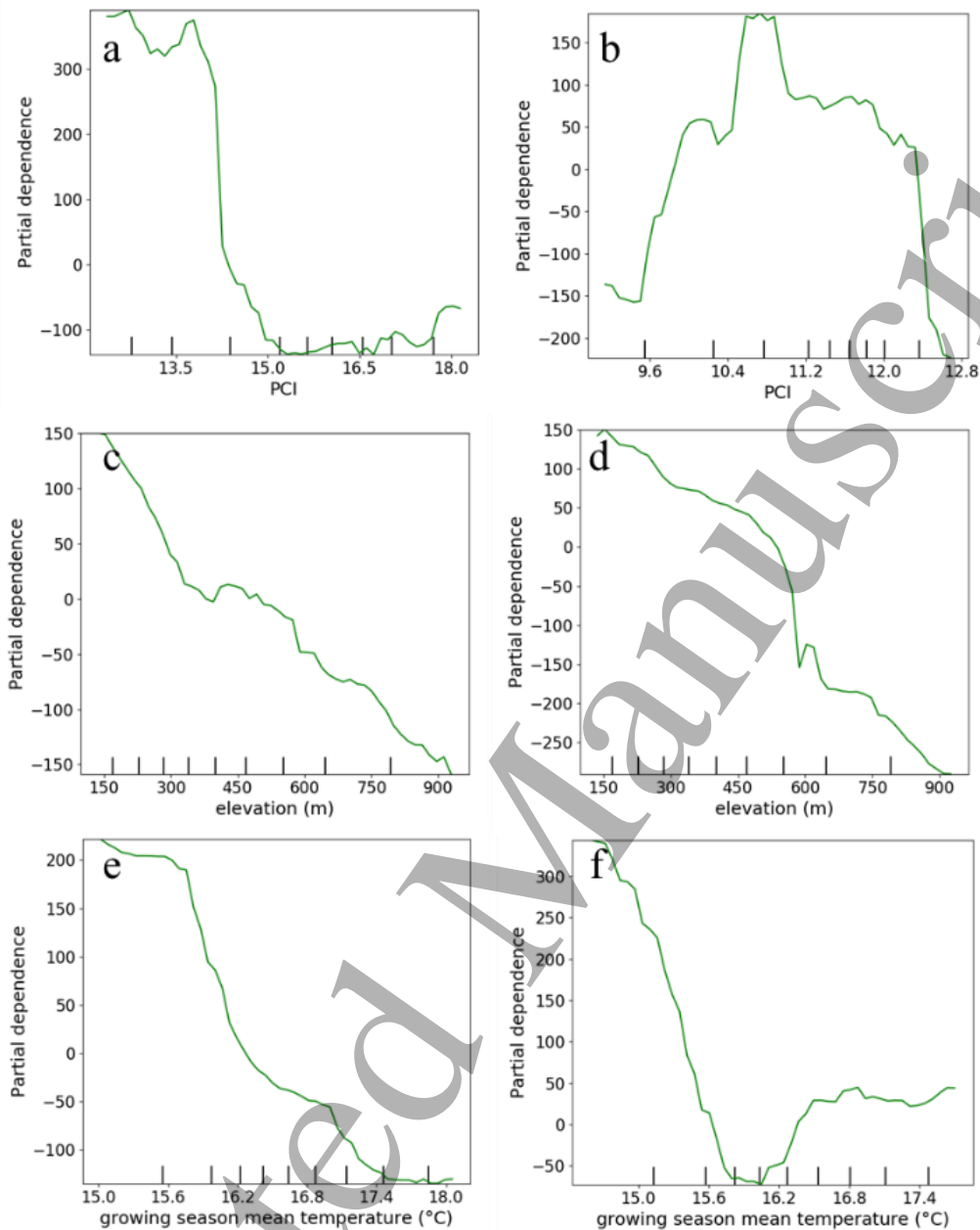
Figure 9. The relative departure from long-term mean production during drought years (a) and wet years (b).

We also found that areas that experienced a smaller forage reduction during drought years were likely to experience a smaller production increase during wet years (Fig. S12c). At a given location, every 1% increase in forage production during wet years corresponded to a 0.55% production reduction during drought years, although the percent increase in precipitation was usually higher in wet years than the percent decrease in drought years (Fig. S12d).

The GBRT models, built separately for wet and dry years, showed different dominant factors controlling the spatial variation of forage productivity. Compared to drought years, the relative importance of precipitation amount decreased from 24 to 19% during wet conditions, while the distribution of precipitation became equally important with precipitation amount (Fig. 6b&c). Soil properties became relatively more important during wet years, i.e., 9.5% as compared to 7.0% in dry years.

Elevation showed a negative impact on forage production under drought conditions, at a rate of -0.36 kg/ha/m (Fig. 10c). Under wet conditions, the reduction in forage production became greater with increasing elevation: -0.33 kg/ha/m at 150-450 m to -0.67 kg/ha/m at 450-900 m (Fig. 10d). Similar to the analysis for the entire time period, lower growing season mean temperature was associated with higher forage production, under dry or wet conditions; however, the influence of growing season mean temperature was stronger for wet years (-336 kg/ha/ $^{\circ}$ C, Fig. 10f) than for drought years

1 (-146 kg/ha/yr/°C, Fig. 10e). The negative influence was most pronounced in cooler
 2 regions (<16 °C, mostly higher elevations, Fig. S13) during wet years (Fig. 10f).



3
 4 Figure 10. Partial dependence of mean forage production during dry years (left) vs. wet
 5 years (right) on (a-b) precipitation concentration index, (c-d) elevation, and (e-f)
 6 growing season mean temperature. These three features show different relationships
 7 with forage production under drought versus wet conditions. Marks on the x-axis
 8 indicate the data distribution.

9 10 **4. Discussion**

11 4.1 Spatial controls on forage production

12 California grassland forage production showed a large degree of spatial variability

1 associated with heterogeneity in environmental conditions. Across the state, climatic
2 factors, especially the amount of precipitation received at the start and end of the
3 growing season, exerted a stronger influence on spatial variability in forage production
4 compared to topography- and soil-related factors. However, there was a strong interplay
5 among factors, with the relative importance of each factor being dependent on local
6 microclimate and climate conditions (Fig. 8).

7 4.1.1 Climate

8 Precipitation in California exhibits large interannual, latitudinal and topographic
9 variation. Consistent with previous studies, our results showed that forage production
10 was a strong function of the total amount and temporal distribution of annual
11 precipitation (Bai et al., 2008; Duncan & Woodmansee, 1975; Sala et al., 1988).
12 Previous studies also suggested that precipitation before November 20th was an
13 important driver of peak forage production at a site in NCCR (Murphy, 1970), as well
14 as demonstrating a significant correlation between peak forage production and
15 November and April precipitation in SNF (Duncan & Woodmansee, 1975).

16 Our results provide robust support for these previous site-level investigations based on
17 14 years of forage production at 30-m resolution across four ecoregions spanning
18 24,000 km². At the statewide scale, our results indicated that November and April
19 precipitation had strong positive impacts on peak forage production. Annual species in
20 California typically germinate in October-November, depending on timing of the
21 germinating rainfall event (Murphy, 1970). Therefore, sufficient precipitation during
22 this period promotes germination and early-season biomass accumulation as residual
23 soil heat and moderate air temperatures allow slow growth. This early season growth
24 increases root and leaf area development that allows for more efficient capture of solar
25 radiation and soil water once temperature and moisture conditions become more
26 favorable later in the growing season (George et al., 2016). Additionally, establishment
27 of early season soil cover may enhance rainfall infiltration into the soil (versus surface
28 runoff), thereby increasing soil water storage for subsequent plant use. In April, as
29 temperatures and solar radiation become more favorable, plants can rapidly accumulate
30 biomass if soil water is available. Therefore, precipitation amounts in November and
31 April appear to contribute a disproportionate increase to annual forage production.

32 Ecoregion-specific modeling revealed precipitation distribution within the growing
33 season as an important factor controlling peak forage production (Fig. 8).
34 Mediterranean annual grasses senesce quickly when soil moisture depletes. Therefore,
35 small but consistent precipitation events throughout the growing season are favorable
36 to higher forage production (Duncan & Woodmansee, 1975). Forage production models
37 for wet-dry endmember conditions revealed that when water is limited during drought
38 years, a more uniformly distributed precipitation regime favors higher forage
39 production (Fig. 10a). In contrast, when soil water is ample during wet years, regions
40 with more uniformly distributed precipitation (PCI<10.8) produced somewhat less
41 forage than regions with more variability in rainfall distribution (Fig. 10b). This
42 observation is likely associated with plants having the highest growth potential when
43 favorable conditions for temperature, solar radiation and precipitation coincide later in
44 the growing season. Therefore, when overall precipitation is higher, greater forage

1 production is achieved when more precipitation occurs during the rapid growing stage,
2 namely April.

3 Temperature affects plant growth through its influence on evapotranspiration and
4 respiration/photosynthetic rates (Vermeire et al., 2009). We found that given the same
5 amount of precipitation, regions with lower daily mean air temperature (T_{mean}) during
6 the growing season had higher forage production (Fig. 7e). This may result in part from
7 warming-caused higher water loss through evaporation, reducing the proportion of
8 'effective precipitation' available for photosynthesis. De Boeck et al. (2006) reported
9 decreased production under warmer situations when comparing grass growth in
10 climate-controlled chambers with ambient and warmer ($+3^{\circ}\text{C}$) temperatures. However,
11 the daily minimum (mostly nighttime) air temperature (T_{min}) showed an opposite effect
12 from T_{mean} (Fig. 7c&e). At nighttime, most plants pause photosynthetic activity and
13 only conduct respiratory activities, consuming carbohydrates. Thus, warmer night
14 temperature increases respiratory C losses (Peraudeau et al., 2015) and photosynthetic
15 capacity during the following day (Turnbull et al., 2002). Our results suggest that when
16 $4.3^{\circ}\text{C} < T_{\text{min}} < 5.4^{\circ}\text{C}$, photosynthetic capacity is more sensitive to changes in nighttime
17 temperature than respiratory capacity, compared with areas with $2.5^{\circ}\text{C} < T_{\text{min}} < 4.3^{\circ}\text{C}$.
18 Our results highlight the different relationships between forage production and air
19 temperature metrics (T_{min} vs. T_{mean}).

20 4.1.2 Topography

21 Landscape positions experiencing less environmental stress (e.g., soil water deficit) are
22 reported to be associated with higher forage production at a ranch with a complex
23 topography (Liu et al., 2019). Our large-scale study here showed that topography
24 contributed only moderately to spatial variability in forage production. Elevation (150
25 to 900 m) was the most influential topography-related factor, with more pronounced
26 impact in the drier CCR and SNF ecoregions. Soil moisture is typically found lower in
27 higher elevations than lower elevation regions at 5-10 cm (Porazinska et al., 2002) and
28 at multiple depths (10 - 90 cm) (Bales et al., 2018) due to less soil development at higher
29 elevations. Higher elevation regions also have higher solar radiation. Together, lower
30 soil moisture and higher solar radiation may invoke additional water stress on forage
31 growth in high elevation regions, and eventually lead to reduced forage production.

32 Aspect and slope showed little impact on forage production, probably because their
33 impacts on insolation are relatively muted prior to the spring solstice and only become
34 more apparent in April, which may enhance the importance of April rainfall on forage
35 growth. In addition to the role in regulating insolation, greater slopes are conducive to
36 greater soil runoff, thereby decreasing water availability for plant use.

37 4.1.3 Soil properties

38 Few studies have considered the role of soil physical properties on California rangeland
39 forage production. Strong impacts from soil pore size distribution and available water
40 holding capacity have been reported for grasslands in the Great Plains (Reyes et al.,
41 2017). However, these grasslands are dominated by perennial species with deep root
42 systems. In parts of California, site-level soil texture and available water holding
43 capacity were reported to be not significantly related to forage production based on an

1 experiment conducted in the NCCR ecoregion (Jones et al., 1983). In our regional
2 analysis, available water holding capacity showed a positive impact on forage
3 production when other variables are held constant. However, spatial variation in soil
4 properties showed a relatively weaker effect on the state-wide variation in long-term
5 mean forage production, compared to climatic factors, solar energy and elevation. On
6 the other hand, we did find soil properties became more important during wetter years
7 (Fig. 6c and Figs 8b-d). Finer textured soils that have higher available water holding
8 capacity are able to retain more rainfall for plant growth (Weng & Luo, 2008). Our
9 findings may be limited by the small variability of plant-available water holding
10 capacity in the upper 25-cm of soils across the study area (e.g., interquartile range=2.7-
11 3.8 cm; CV=27%). Further, the rooting distribution of annual grasses/forbs is
12 concentrated in the upper 15 cm with few roots extending below a depth of 30 cm,
13 thereby limiting the importance of soil water storage in controlling overall annual
14 forage production relative to more deeply rooted perennials (Gordon & Rice, 1992;
15 Holmes & Rice, 1996).

16 The weak relationship between soil properties and forage production is not equivalent
17 to low importance of soil moisture. Soil moisture not only controls onset of the growing
18 season (Bart, Tague, & Dennison, 2017), but also is positively related to annual forage
19 production (Becchetti et al., 2016). Additionally, soil water storage serves as a water
20 buffer to support plant growth between rainfall events; therefore, periodic rainfall
21 events that are well distributed throughout the season are important for sustaining soil
22 water and forage growth over longer time periods.

23 4.2 Implications for land managers and policymakers

24 Sustainable management of forage resources is a critical goal for rangeland livestock
25 producers (Kachergis et al., 2013; Roche et al., 2015) and a key factor in adaptive
26 rangeland decision-making (Roche, 2016). Stakeholders make decisions at different
27 time scales, depending on their management goals (Brown et al., 2017). For example,
28 strategic planning for ranch sustainability may require long-term mean and wet-dry year
29 variability information, while tactical planning, such as rapid drought response,
30 depends on near real time information. Annual forage forecasts could help land
31 managers make decisions about grazing and stocking rate strategies, such as taking
32 proactive actions before dry or drought conditions fully emerge. Our results suggest
33 spatial variability in forage production is more responsive to precipitation received in
34 November and April. Consequently, November precipitation could be used as an
35 indicator to estimate potential annual forage production using our machine learning
36 model, assuming other factors are at multiyear mean levels. Noting that for ranches in
37 mesic regions (e.g., NCCR), accuracy of this method could be lower than in arid regions
38 because precipitation amount is not the only factor influencing forage production.

39 Annual forage prediction maps and identified key drivers from this study also inform
40 policy decision-making. For example, the estimated forage production maps and
41 modeling results at 30 m could inform drought-monitoring efforts in near real-time,
42 providing a low cost, objective and large-scale assessment of California rangeland
43 forage conditions. The US Drought Monitor (USDM,
44 <https://droughtmonitor.unl.edu/About/WhatistheUSDM.aspx>) is a multi-institutional effort

1 that provides drought classification maps to assess and identify drought conditions each
2 week across the country (Svoboda et al., 2002). Because of their coarse spatial
3 resolution, USDM maps have limited utility for drought mitigation at more localized
4 scales (Brown et al., 2008). The USDM approach is mostly based on weather data
5 coupled with expert inputs from resource agencies (Svoboda et al., 2002), and does not
6 explicitly consider differences in plant response to drought. Our study demonstrated
7 large variations in forage production departure during drought years, suggesting the
8 importance of including perspectives of plant sensitivity to drought when mapping
9 drought intensity. The Vegetation Drought Response (VegDRI) tool provides a
10 satellite-based indication of drought effects on vegetation health at 1-km resolution (J.
11 F. Brown et al., 2008). VegDRI maps are limited by a lack of extensive ground truthing
12 (e.g., green biomass), which could be remedied using our estimated forage production
13 maps.

14 Finally, this work can inform implementation of drought relief and disaster payment
15 programs, such as the Livestock Forage Program (LFP) and Noninsured Crop Disaster
16 Assistance Program (NAP) by USDA. The LFP is currently triggered by USDM ratings
17 and duration of forage production loss at the county level. However, our results
18 demonstrate that reductions in forage production vary significantly during drought
19 within an individual county (Fig. 9). Further, our calibrated cumulative APAR based
20 LUE method could generate near real-time forage production maps at 30-m resolution.
21 These maps provide finer spatial resolution information directly related to forage
22 productivity. With this higher resolution information, it is possible to declare sub-
23 county production-based drought, which would allow disaster relief programs to better
24 distribute resources (George et al., 2010). Our results also complement existing
25 rangeland production monitoring tools, such as Grass-Cast (<https://grasscast.unl.edu/>),
26 that are focused on the Great Plains and Southwest regions. Our quantified relationships
27 between forage production and its key driver may provide opportunities to expand such
28 tools to larger geographic areas.

29 4.3 Implications for assessing climate change impacts

30 Temperature is projected to warm 1.7-5.8 °C over the next century in California (Cayan
31 et al., 2012), with much of the increase resulting from rising minimum temperatures
32 (mostly nighttime) (Cordero et al., 2011). Our study indicated forage production
33 responds differently to changes in minimum temperature (positive when $T_{\min} > 4.3^{\circ}\text{C}$)
34 versus average temperature (negative) (Fig. 7c&d). Therefore, an increase in minimum
35 temperature and average temperature may produce contrasting site-specific effects on
36 forage production. Previous studies forecasting climate change impacts on forage
37 production did not account for different responses to rising minimum versus average
38 temperatures (Zavaleta et al., 2003). A California annual grassland field study found
39 experimental warming reduced canopy greenness (Zavaleta et al., 2003); however,
40 these results may not reflect actual warming effects because the same intensity of
41 warming was applied during both day and nighttime periods. A climate change impact
42 modeling study for the San Francisco Bay area suggested that rangeland forage
43 production may be enhanced by future temperature and precipitation conditions
44 (Chaplin-Kramer & George, 2013). Yet, this conclusion was based on a growing
45 degree-day model to forecast future forage production and did not account for

1 differential rising rates between maximum and minimum temperatures.

2 Precipitation varies greatly from year-to-year in California and is expected to become
3 more variable and unpredictable in the future (Cayan et al., 2012). Extremely wet and
4 dry years are likely to appear more frequently in the future. Forage production showed
5 different resilience towards extreme precipitation conditions across the study area.
6 Mesic regions exhibited a smaller departure from the LTM than drier regions under
7 drought or wet conditions (Fig. 10a&b). This spatially varying response to changes in
8 precipitation suggest that forage production in more arid regions may get hit harder by
9 climate change than more mesic regions. Our findings are in general agreement with
10 previous climate change sensitivity analyses examining forage production under a
11 Mediterranean climate (Golodets et al., 2013; Huxman et al., 2004). In the meantime,
12 impacts from more frequent drought may be more severe than predicted because of the
13 predicted rising temperature (Polley et al., 2017). Some ranchers may be forced to
14 switch to livestock species that are more adapted to warm temperatures and drought,
15 such as sheep or goats (Kay, 1997).

16 **5. Conclusion**

17 We investigated relationships between long-term mean forage production and key
18 factors driving forage production across four California ecoregions (~24,000 km²).
19 We explored 41 potential variables derived from climate, topography and soil
20 properties that were reduced to 11 feature groups to avoid collinearity. Together, these
21 11 features explained 67% of the variation in annual forage production across the
22 study area. Precipitation was the dominant driver for forage production with high
23 sensitivity to November (germination) and April (rapid growth period) precipitation
24 amounts. The influence of precipitation amount was most pronounced during drought
25 years and in drier ecoregions (CCR&SNF); in wet years and wetter ecoregions
26 (NCCR&NCICR) other variables such as precipitation distribution and solar energy
27 showed a relatively stronger control. Minimum air temperature showed an increased
28 effect in wetter ecoregions, but not during wet years. Elevation showed the strongest
29 impact among topography factors with higher elevations having lower forage
30 production. Soil properties showed the least influence among predictor variables,
31 which is possibly due to their small degree of variability across the study area. The
32 quantified linkages and forage production maps provide important decision-making
33 information for rangeland managers and state-wide drought-disaster relief programs.
34 Our approach has the ability to forecast forage production in near real-time to provide
35 rangeland managers with information to make proactive grazing decisions, especially
36 with regard to drought-induced risks. We anticipate that future research will build
37 upon this approach as new remote sensing platforms become available to monitor
38 abiotic (e.g., soil moisture) and biotic controls of forage production in near real-time.
39 This work also provides a foundation for predicting rangeland forage response to
40 future climate change scenarios at regional scales.

41

42 **Acknowledgements**

43 This work was supported by Russell L. Rustici Rangeland and Cattle Research Endowment.

1 We thank Nikolas Schweitzer, Alison Smith, Sarah Covello, Mui Lay, Andy Wong, Scott
 2 Devine, and Karl Linsteadt for their help with collecting field measurements. We especially
 3 thank Royce Larsen for logistical support and guidance in selecting and maintain field sites.

4 5 Reference

6 Akitsu, T., Kume, A., Hirose, Y., Ijima, O., & Nasahara, K. N. (2015). On the Stability
 7 of Radiometric Ratios of Photosynthetically Active Radiation to Global Solar
 8 Radiation in Tsukuba, Japan. *Agricultural and Forest Meteorology*, 209, 59–68.
 9 <https://doi.org/10.1016/j.agrformet.2015.04.026>

10 Asner, G. P., Brodrick, P. G., Anderson, C. B., Vaughn, N., Knapp, D. E., & Martin, R.
 11 E. (2016). Progressive Forest Canopy Water Loss During the 2012–2015
 12 California Drought. *Proceedings of the National Academy of Sciences*, 113(2),
 13 E249–E255.

14 Bai, Y., Wu, J., Xing, Q., Pan, Q., Huang, J., Yang, D., & Han, X. (2008). Primary
 15 Production and Rain Use Efficiency Across a Precipitation Gradient on the
 16 Mongolia Plateau. *Ecology*, 89(8), 2140–2153. <https://doi.org/10.1890/07-0992.1>

17 Bales, R. C., Stacy, E. M., Meng, X., Conklin, M. H., Kirchner, P. B., & Zheng, Z.
 18 (2018). Spatially Distributed Water-balance and Meteorological Data from the
 19 Wolverton Catchment, Sequoia National Park, California. *Earth System Science*
 20 *Data*, 10(4), 2115–2122. <https://doi.org/10.5194/essd-10-2115-2018>

21 Bart, R. R., Tague, C. L., & Dennison, P. E. (2017). Modeling Annual Grassland
 22 Phenology Along the Central Coast of California. *Ecosphere*, 8(7), e01875.
 23 <https://doi.org/10.1002/ecs2.1875>

24 Bartolome, J. W., Barry, W. J., Griggs, T., & Hopkinson, P. (2007). Valley Grassland.
 25 *Terrestrial Vegetation of California.*, 31(Heady 1977), 432.
 26 <https://doi.org/10.2307/2806144>

27 Beaudette, D. E., Roudier, P., & O'Geen, A. T. (2013). Algorithms for Quantitative
 28 Pedology: A Toolkit for Soil Scientists. *Computers & Geosciences*, 52, 258–268.

29 Becchetti, T., George, M., McDougald, N., Dudley, D. M., Connor, M., Flavell, D.
 30 K., ... Markegard, G. (2016). Annual Range Forage Production. *University of*
 31 *California Agriculture and Natural Resources Publication*, 8018(3), 1–12.
 32 Retrieved from <http://ahrcatalog.ucanr.edu/pdf/8018.pdf>

33 Blackburn, W. J., & Proctor, J. T. A. (1983). Estimating Photosynthetically Active
 34 Radiation from Measured Solar Irradiance. *Solar Energy*, 3183(2), 233–234.

35 Boschetti, M., Bocchi, S., & Brivio, P. A. (2007). Assessment of Pasture Production in
 36 the Italian Alps using Spectrometric and Remote Sensing Information. *Agriculture,*
 37 *Ecosystems & Environment*, 118(1–4), 267–272.

38 Breiman, L., Friedman, J., Stone, C. J., & Olshen, R. A. (1984). *Classification and*
 39 *Regression Trees*. CRC press.

40 Brown, J., Alvarez, P., Byrd, K., Deswood, H., Elias, E., & Spiegel, S. (2017). Coping
 41 With Historic Drought in California Rangelands: Developing a More Effective
 42 Institutional Response. *Rangelands*, 39(2), 73–78.

- 1 <https://doi.org/10.1016/j.rala.2017.01.002>
- 2 Brown, J. F., Wardlow, B. D., Tadesse, T., Hayes, M. J., & Reed, B. C. (2008). The
3 Vegetation Drought Response Index (VegDRI): A New Integrated Approach for
4 Monitoring Drought Stress in Vegetation. *GIScience & Remote Sensing*, 45(1),
5 16–46.
- 6 California Department of Food & Agriculture. (2015). *2015 Crop Year Report*.
7 Sacramento. Retrieved from <https://www.cdfa.ca.gov/statistics/>
- 8 Carlson, T. N., & Ripley, D. A. (1997). On the relation between NDVI, fractional
9 vegetation cover, and leaf area index. *Remote Sensing of Environment*, 62(3), 241–
10 252.
- 11 Cayan, D., Tyree, M., Pierce, D., & Das, T. (2012). *Climate Change and Sea Level Rise*
12 *Scenarios for California Vulnerability and Adaptation Assessment: A White Paper*
13 *from the California Energy Commission's California Climate Change Center*.
14 *California Energy Commission*. Retrieved from
15 [http://www.energy.ca.gov/2012publications/CEC-500-2012-008/CEC-500-2012-](http://www.energy.ca.gov/2012publications/CEC-500-2012-008/CEC-500-2012-008.pdf)
16 [008.pdf](http://www.energy.ca.gov/2012publications/CEC-500-2012-008/CEC-500-2012-008.pdf)
- 17 Chaplin-Kramer, R., & George, M. R. (2013). Effects of Climate Change on Range
18 Forage Production in the San Francisco Bay Area. *PLoS ONE*, 8(3), 1–11.
19 <https://doi.org/10.1371/journal.pone.0057723>
- 20 Chen, B., Huang, B., & Xu, B. (2015). Comparison of Spatiotemporal Fusion Models:
21 A Review. *Remote Sensing*, 7(2), 1798–1835. <https://doi.org/10.3390/rs70201798>
- 22 Chen, J., Jönsson, P., Tamura, M., Gu, Z., Matsushita, B., & Eklundh, L. (2004). A
23 Simple Method for Reconstructing a High-quality NDVI Time-series Data Set
24 Based on the Savitzky-Golay Filter. *Remote Sensing of Environment*, 91(3–4),
25 332–344. <https://doi.org/10.1016/j.rse.2004.03.014>
- 26 Cleland, D. T., Freeouf, J. A., Keys, J. E., Nowacki, G. J., Carpenter, C. A., & McNab,
27 W. H. (2007). Ecological Subregions: Sections and Subsections for the
28 Conterminous United States. *General Technical Report WO-76D*, 76.
- 29 Cordero, E. C., Kessomkiat, W., Abatzoglou, J., & Mauget, S. A. (2011). The
30 Identification of Distinct Patterns in California Temperature Trends. *Climatic*
31 *Change*, 108(1), 357–382. <https://doi.org/10.1007/s10584-011-0023-y>
- 32 De Boeck, H. J., Lemmens, C. M. H. M., Bossuyt, H., Malchair, S., Carnol, M., Merckx,
33 R., ... Ceulemans, R. (2006). How Do Climate Warming and Plant Species
34 Richness Affect Water Use in Experimental Grasslands? *Plant and Soil*, 288(1–2),
35 249–261. <https://doi.org/10.1007/s11104-006-9112-5>
- 36 Deering, D. W., Rouse, J. W., Haas, R. H., & Schell, J. A. (1975). Measuring Forage
37 Production of Grazing Units from Landsat MSS Data. In *10th Symposium on*
38 *Remote Sensing of Environment* (pp. 1169–1178). Ann Arbor: ERIM.
- 39 Devine, S. M., O'Geen, A. T., Larsen, R. E., Dahlke, H. E., Liu, H., Jin, Y., & Dahlgren,
40 R. A. (2019). Microclimate–forage Growth Linkages Across Two Strongly
41 Contrasting Precipitation Years in a Mediterranean Catchment. *Ecohydrology*,
42 12(8). <https://doi.org/10.1002/eco.2156>
- 43 Duncan, D. A., & Woodmansee, R. G. (1975). Forecasting Forage Yield from

- 1
2
3
4
5
6
7
8
9
10
11
12
13
14
15
16
17
18
19
20
21
22
23
24
25
26
27
28
29
30
31
32
33
34
35
36
37
38
39
40
41
42
43
44
45
46
47
48
49
50
51
52
53
54
55
56
57
58
59
60
- 1 Precipitation in California's Annual Rangeland. *Journal of Range Management*,
2 327–329.
- 3 Dwyer, J. L., Roy, D. P., Sauer, B., Jenkerson, C. B., Zhang, H. K., & Lymburner, L.
4 (2018). Analysis Ready Data: Enabling Analysis of the Landsat Archive. *Remote*
5 *Sensing*, 10(9), 1363. <https://doi.org/10.3390/rs10091363>
- 6 Friedman, J. H. (2001). Greedy Function Approximation: A Gradient Boosting
7 Machine. *Annals of Statistics*, 29(5), 1189–1232. <https://doi.org/10.2307/2699986>
- 8 Fuhlendorf, S. D., Fynn, R. W. S., McGranahan, D. A., & Twidwell, D. (2017).
9 Heterogeneity as the Basis for Rangeland Management (pp. 169–196). Springer,
10 Cham. https://doi.org/10.1007/978-3-319-46709-2_5
- 11 Gaffney, R., Porensky, L. M., Gao, F., Irisarri, J. G., Durante, M., Derner, J. D., &
12 Augustine, D. J. (2018). Using APAR to Predict Aboveground Plant Productivity
13 in Semi-Arid Rangelands: Spatial and Temporal Relationships Differ. *Remote*
14 *Sensing*, 10(9). <https://doi.org/10.3390/rs10091474>
- 15 Gao, F., Masek, J., Schwaller, M., & Hall, F. (2006). On the Blending of The landsat
16 and MODIS Surface Reflectance: Predicting Daily Landsat Surface Reflectance.
17 *IEEE Transactions on Geoscience and Remote Sensing*, 44(8), 2207–2218.
18 <https://doi.org/10.1109/TGRS.2006.872081>
- 19 Gao, Q., Zhu, W., Schwartz, M. W., Ganjurjav, H., Wan, Y., Qin, X., ... Li, Y. (2016).
20 Climatic Change Controls Productivity Variation in Global Grasslands. *Scientific*
21 *Reports*, 6(1), 1–10. <https://doi.org/10.1038/srep26958>
- 22 George, M., Bartolome, J., McDougald, N., Connor, M., Vaughn, C., & Markegard, G.
23 (2016). Annual Range Forage Production. *Rangeland Management Series*,
24 8018(Table 1), 1–9.
- 25 George, M. R. R., Larsen, R. E. E., McDougald, N. M. M., Vaughn, C. E. E., Flavell,
26 D. K. K., Dudley, D. M. M., ... Forero, L. C. C. (2010). Determining Drought on
27 California's Mediterranean-type Rangelands: The Noninsured Crop Disaster
28 Assistance Program. *Rangelands*, 32(3), 16–20.
29 <https://doi.org/10.2111/RANGELANDS-D-10-00003.1>
- 30 George, M. R., Raguse, C. A., Clawson, W. J., Wilson, C. B., Willoughby, R. L.,
31 McDougald, N. K., ... Murphy, A. H. (1988). Correlation of Degree-Days with
32 Annual Herbage Yields and Livestock Gains. *Journal of Range Management*,
33 41(3). <https://doi.org/10.2307/3899166>
- 34 George, M. R., Williams, W. A., McDougald, N. K., Clawson, W. J., & Murphy, A. H.
35 (1989). Predicting Peak Standing Crop on Annual Range Using Weather Variables.
36 *Journal of Range Management*, 42(6), 508–512. <https://doi.org/10.2307/3899238>
- 37 Ghosh, S. (2019). Droughts and Water Trading in the Western United States: Recent
38 Economic Evidence. *International Journal of Water Resources Development*,
39 35(1), 145–159.
- 40 Golodets, C., Sternberg, M., Kigel, J., Boeken, B., Henkin, Z., Seligman, N. G., &
41 Ungar, E. D. (2013). From Desert to Mediterranean Rangelands: Will Increasing
42 Drought and Inter-annual Rainfall Variability Affect Herbaceous Annual Primary
43 Productivity? *Climatic Change*, 119(3–4), 785–798.

- 1 <https://doi.org/10.1007/s10584-013-0758-8>
- 2 Gordon, D. R., & Rice, K. J. (1992). Partitioning of Space and Water between Two
3 California Annual Grassland Species. *American Journal of Botany*, 79(9), 967–
4 976.
- 5 Hart, Q. J., Brugnach, M., Temesgen, B., Rueda, C., Ustin, S. L., & Frame, K. (2009).
6 Daily Reference Evapotranspiration for California using Satellite Imagery and
7 Weather Station Measurement Interpolation. *Civil Engineering and*
8 *Environmental Systems*, 26(1), 19–33.
9 <https://doi.org/10.1080/10286600802003500>
- 10 Hay, J. E. (1993). Satellite Based Estimates of Solar Irradiance at The Earth's Surface—
11 I. Modelling Approaches. *Renewable Energy*, 3(4/5), 381–393. Retrieved from
12 <https://www.sciencedirect.com/science/article/pii/096014819390105P>
- 13 Holmes, T. H., & Rice, K. J. (1996). Patterns of Growth and Soil-Water Utilization in
14 Some Exotic Annuals and Native Perennial Bunchgrasses of California. *Annals of*
15 *Botany*, 78(2), 233–243.
- 16 Hufstader, R. W. (1978). Growth Rates and Phenology of Some Southern California
17 Grassland Species. *Journal of Range Management*, 31(6), 465–466. Retrieved
18 from <https://journals.uair.arizona.edu/index.php/jrm/article/viewFile/6887/6497>
- 19 Huxman, T. E., Smith, M. D., Fay, P. A., Knapp, A. K., Shaw, M. R., Lolk, M. E., ...
20 Williams, D. G. (2004). Convergence Across Biomes to a Common Rain-Use
21 Efficiency. *Nature*, 429(6992), 651–654. <https://doi.org/10.1038/nature02561>
- 22 Jackson, R. D., & Bartolome, J. W. (2007). Grazing Ecology of California Grasslands.
23 In M. Stromberg (Ed.), *California Grasslands: Ecology and Management* (pp.
24 197–206). University of California Press Berkeley, CA.
- 25 Jenson, S. K., & Domingue, J. O. (1988). Extracting Topographic Structure from
26 Digital Elevation Data for Geographic Information System Analysis.
27 *Photogrammetric Engineering and Remote Sensing*, 54(11), 1593–1600.
- 28 Jin, Y., & Goulden, M. L. (2014). Ecological Consequences of Variation in
29 Precipitation: Separating Short- versus Long-Term Effects using Satellite Data.
30 *Global Ecology and Biogeography*, 23(3), 358–370.
31 <https://doi.org/10.1111/geb.12135>
- 32 Jones, M. B., Williams, W. A., & Vaughn, C. E. (1983). Soil Characteristics Related to
33 Production on Subclover-grass Range *Trifolium Subterraneum*, in Coastal
34 California. *Rangeland Ecology & Management/Journal of Range Management*
35 *Archives*, 36(4), 444–446.
- 36 Jones, M. O., Allred, B. W., Naugle, D. E., Maestas, J. D., Donnelly, P., Metz, L. J., ...
37 McIver, J. D. (2018). Innovation in Rangeland Monitoring: Annual, 30 m, Plant
38 Fu1. Jones, M.O.; Allred, B.W.; Naugle, D.E.; Maestas, J.D.; Donnelly, P.; Metz,
39 L.J.; Karl, J.; Smith, R.; Bestelmeyer, B.; Boyd, C.; Kerby, J.D.; McIver, J.D.
40 Innovation in Rangeland Monitoring: An. *Ecosphere*, 9(9), e02430.
41 <https://doi.org/10.1002/ecs2.2430>
- 42 Kachergis, E., Derner, J., Roche, L., Tate, K., Lubell, M., Meador, R., & Magagna, J.
43 (2013). Characterizing Wyoming Ranching Operations: Natural Resource Goals,

- 1 Management Practices and Information Sources. *Natural Resources*, 4, 45–54.
2 <https://doi.org/10.4236/nr.2013.41005>
- 3 Kay, R. N. B. (1997). Responses of African Livestock and Wild Herbivores to Drought.
4 *Journal of Arid Environments*, 37(4), 683–694.
- 5 Larsen, R., Striby, K., & Horney, M. (2014). Fourteen Years of Frage Monitoring on
6 the California Central Coast Shows Tremendous Variation. *Proceedings of the 7th*
7 *California Oak Symposium: Managing Oak Woodlands in a Dynamic World*,
8 *PSW-GTR-25*, 273–281.
- 9 Le Houerou, H. N. (1984). Rain Use Efficiency: A Unifying Concept in Arid-land
10 Ecology. *Journal of Arid Environments*, 7(3), 213–247.
- 11 Li, R., Zhao, L., Ding, Y., Wang, S., Ji, G., Xiao, Y., ... Sun, L. (2010). Monthly Ratios
12 of PAR to Global Solar Radiation Measured at Northern Tibetan Plateau, China.
13 *Solar Energy*, 84(6), 964–973. Retrieved from
14 <http://www.sciencedirect.com/science/article/pii/S0038092X1000109X>
- 15 Liu, H., Dahlgren, R., Larsen, R., Devine, S., Roche, L., O' Geen, A., ... Jin, Y. (2019).
16 Estimating Rangeland Forage Production Using Remote Sensing Data from a
17 Small Unmanned Aerial System (sUAS) and PlanetScope Satellite. *Remote*
18 *Sensing*, 11(5), 595. <https://doi.org/10.3390/rs11050595>
- 19 Los, S. O., Pollack, N. H., Parris, M. T., Collatz, G. J., Tucker, C. J., Sellers, P. J., ...
20 Dazlich, D. a. (2000). A Global 9-yr Biophysical Land Surface Dataset from
21 NOAA AVHRR Data. *Journal of Hydrometeorology*, 1(2), 183–199.
22 [https://doi.org/10.1175/1525-7541\(2000\)001<0183:AGYBLS>2.0.CO;2](https://doi.org/10.1175/1525-7541(2000)001<0183:AGYBLS>2.0.CO;2)
- 23 Macon, D. K., Barry, S., Becchetti, T., Davy, J. S., Doran, M. P., Finzel, J. A., ... Roche,
24 L. M. (2016). Coping With Drought on California Rangelands. *Rangelands*, 38(4),
25 222–228. <https://doi.org/10.1016/j.rala.2016.06.005>
- 26 Molnar, C. (2019). *Interpretable Machine Learning. A Guide for Making Black Box*
27 *Models Explainable*. Retrieved from [https://christophm.github.io/interpretable-](https://christophm.github.io/interpretable-ml-book/)
28 [ml-book/](https://christophm.github.io/interpretable-ml-book/)
- 29 Murphy, A. H. (1970). Predicted Forage Yield Based on Fall Precipitation in California
30 Annual Grasslands. *Journal of Range Management*, 23(5), 363–365.
31 <https://doi.org/10.2307/3896168>
- 32 O'Geen, A., Walkinshaw, M., & Beaudette, D. (2017). SoilWeb: A Multifaceted
33 Interface to Soil Survey Information. *Soil Science Society of America Journal*,
34 81(4), 853–862.
- 35 Oliver, J. E. (1980). Monthly Precipitation Distribution: A Comparative Index.
36 *Professional Geographer*, 32(3), 300–309. [https://doi.org/10.1111/j.0033-](https://doi.org/10.1111/j.0033-0124.1980.00300.x)
37 [0124.1980.00300.x](https://doi.org/10.1111/j.0033-0124.1980.00300.x)
- 38 Papaioannou, G., Papanikolaou, N., & Retalis, D. (1993). Relationships of
39 Photosynthetically Active Radiation and Shortwave Irradiance. *Theoretical and*
40 *Applied Climatology*, 48(1), 23–27. Retrieved from
41 <http://link.springer.com/article/10.1007/BF00864910>
- 42 Parton, W., Morgan, J., Smith, D., Del Grosso, S., Prihodko, L., Lecain, D., ... Lutz, S.
43 (2012). Impact of Precipitation Dynamics on Net Ecosystem Productivity. *Global*

- 1
2
3
4
5
6
7
8
9
10
11
12
13
14
15
16
17
18
19
20
21
22
23
24
25
26
27
28
29
30
31
32
33
34
35
36
37
38
39
40
41
42
43
44
45
46
47
48
49
50
51
52
53
54
55
56
57
58
59
60
- 1 *Change Biology*, 18(3), 915–927. <https://doi.org/10.1111/j.1365-2486.2011.02611.x>
- 3 Pedregosa, F., Varoquaux, G., Gramfort, A., Michel, V., Thirion, B., Grisel, O., ...
4 Dubourg, V. (2011). Scikit-learn: Machine learning in Python. *The Journal of*
5 *Machine Learning Research*, 12, 2825–2830.
- 6 Peraudeau, S., Lafarge, T., Roques, S., Quiñones, C. O., Clement-Vidal, A., Ouwerkerk,
7 P. B. F., ... Dingkuhn, M. (2015). Effect of Carbohydrates and Night Temperature
8 on Night Respiration in Rice. *Journal of Experimental Botany*, 66(13), 3931–3944.
9 <https://doi.org/10.1093/jxb/erv193>
- 10 Pitt, M. D., & Heady, H. F. (1978). Responses of Annual Vegetation to Temperature
11 and Rainfall Patterns in Northern California. *Ecology*, 59(2), 336–350.
12 <https://doi.org/10.2307/1936378>
- 13 Polley, W., Bailey, D., Nowak, R., & Stafford-Smith, M. (2017). Ecological
14 Consequences of Climate Change on Rangelands. In *Rangeland Systems* (pp. 229–
15 260). Springer. <https://doi.org/10.1007/978-3-319-46709-2>
- 16 Porazinska, D. L., Wall, D. H., & Virginia, R. A. (2002). Population age structure of
17 nematodes in the Antarctic Dry Valleys: Perspectives on time, space, and habitat
18 suitability. *Arctic, Antarctic, and Alpine Research*, 34(2), 159–168.
19 <https://doi.org/10.2307/1552467>
- 20 Rabus, B., Eineder, M., Roth, A., & Bamler, R. (2003). The Shuttle Radar Topography
21 Mission—A New Class of Digital Elevation Models Acquired by Spaceborne
22 Radar. *ISPRS Journal of Photogrammetry and Remote Sensing*, 57(4), 241–262.
- 23 Reeves, M. C., Robert, A., Angerer, J., Hunt Jr, E. R., Wasantha, R., & Kumar, L.
24 (2015). Global View of Remote Sensing of Rangelands: Evolution, Applications,
25 Future Pathways. In *Land Resources Monitoring, Modeling, and Mapping with*
26 *Remote Sensing* (pp. 237–266). Boca Raton, FL: CRC Press/Taylor and Francis
27 Group.
- 28 Reyes, J. J., Tague, C. L., Evans, R. D., & Adam, J. C. (2017). Assessing the Impact of
29 Parameter Uncertainty on Modeling Grass Biomass Using a Hybrid Carbon
30 Allocation Strategy. *Journal of Advances in Modeling Earth Systems*, 9(8), 2968–
31 2992. <https://doi.org/10.1002/2017MS001022>
- 32 Roche, L. M. (2016). Adaptive Rangeland Decision-Making and Coping with Drought.
33 *Sustainability*, 8(12), 1334.
- 34 Roche, L. M., Schohr, T. K., Derner, J. D., Lubell, M. N., Cutts, B. B., Kachergis, E., ...
35 Tate, K. W. (2015). Sustaining Working Rangelands: Insights from Rancher
36 Decision Making. *Rangeland Ecology & Management*, 68(5), 383–389.
37 <https://doi.org/10.1016/J.RAMA.2015.07.006>
- 38 Sala, O. E., Parton, W. J., Joyce, L. A., & Lauenroth, W. K. (1988). Primary Production
39 of the Central Grassland Region of the United States. *Ecology*, 69(1), 40–45.
- 40 Schohr, T. (2014). *Sustaining Multifunctional Working Rangelands: Social, Economic,*
41 *and Ecological Insights into Rancher Decision-Making*. Retrieved from
42 <http://gradworks.umi.com/15/65/1565728.html>
- 43 Sellers, P. J., Los, S. O., Tucker, C. J., Justice, C. O., Dazlich, D. A., Collatz, G. J., &

- 1
2
3
4
5
6
7
8
9
10
11
12
13
14
15
16
17
18
19
20
21
22
23
24
25
26
27
28
29
30
31
32
33
34
35
36
37
38
39
40
41
42
43
44
45
46
47
48
49
50
51
52
53
54
55
56
57
58
59
60
- 1 Randall, D. A. (1996). A Revised Land Surface Parameterization (SiB2) Ffor
2 Atmospheric GCMs. Part II: The Generation of Global Fields of Terrestrial
3 Biophysical Parameters from Datellite Data. *Journal of Climate*, 9(4), 706–737.
4 [https://doi.org/10.1175/1520-0442\(1996\)009<0706:ARLSPF>2.0.CO;2](https://doi.org/10.1175/1520-0442(1996)009<0706:ARLSPF>2.0.CO;2)
- 5 Sloat, L. L., Gerber, J. S., Samberg, L. H., Smith, W. K., Herrero, M., Ferreira, L. G., ...
6 West, P. C. (2018). Increasing Importance of Precipitation Variability on Global
7 Livestock Grazing Lands. *Nature Climate Change*, 8(3), 214–218.
8 <https://doi.org/10.1038/s41558-018-0081-5>
- 9 Svoboda, M., LeComte, D., Hayes, M., Heim, R., Gleason, K., Angel, J., ... Stooksbury,
10 D. (2002). The Drought Monitor. *Bulletin of the American Meteorological Society*,
11 83(8), 1181–1190.
- 12 Tan, B., Masek, J. G., Wolfe, R., Gao, F., Huang, C., Vermote, E. F., ... Ederer, G.
13 (2013). Improved Forest Change Detection with Terrain Illumination Corrected
14 Landsat Images. *Remote Sensing of Environment*, 136, 469–483.
15 <https://doi.org/10.1016/j.rse.2013.05.013>
- 16 Thornton, P. E., Thornton, M. M., Mayer, B. W., Wei, Y., Devarakonda, R., Vose, R.
17 S., & Cook, R. B. (2016). Daymet: Daily Surface Weather Data on a 1-km Grid
18 for North America, Version 3. ORNL Distributed Active Archive Center.
19 <https://doi.org/10.3334/ORNLDAAC/1328>
- 20 Turnbull, M. H., Murthy, R., & Griffin, K. L. (2002). The Relative Impacts of Daytime
21 and Night-Time Warming on Photosynthetic Capacity in *Populus Deltoides*. *Plant,*
22 *Cell and Environment*, 25(12), 1729–1737. [https://doi.org/10.1046/j.1365-](https://doi.org/10.1046/j.1365-3040.2002.00947.x)
23 [3040.2002.00947.x](https://doi.org/10.1046/j.1365-3040.2002.00947.x)
- 24 Vermeire, L. T., Heitschmidt, R. K., & Rinella, M. J. (2009). Primary Productivity and
25 Precipitation-use Efficiency in Mixed-grass Prairie: A Comparison of Northern
26 and Southern US Sites. *Rangeland Ecology & Management*, 62(3), 230–239.
- 27 Weng, E., & Luo, Y. (2008). Soil Hydrological Properties Regulate Grassland
28 Ecosystem Responses to Multifactor Global Change: A Modeling Analysis.
29 *Journal of Geophysical Research*, 113(G3), G03003.
30 <https://doi.org/10.1029/2007JG000539>
- 31 Williams, A. P., Seager, R., Abatzoglou, J. T., Cook, B. I., Smerdon, J. E., & Cook, E.
32 R. (2015). Contribution of Anthropogenic Warming to California Drought during
33 2012–2014. *Geophysical Research Letters*, 42(16), 6819–6828.
- 34 Willms, W. D. (1988). Forage Production and Utilization in Various Topographic
35 Zones of the Fescue Grasslands. *Canadian Journal of Animal Science*, 68(1), 211–
36 223.
- 37 Xu, B., Yang, X. C., Tao, W. G., Qin, Z. H., Liu, H. Q., Miao, J. M., & Bi, Y. Y. (2008).
38 MODIS-based Remote Sensing Monitoring of Grass Production in China.
39 *International Journal of Remote Sensing*, 29(17–18), 5313–5327.
- 40 Zavaleta, E. S., Thomas, B. D., Chiariello, N. R., Asner, G. P., Shaw, M. R., & Field,
41 C. B. (2003). Plants Reverse Warming Effect on Ecosystem Water Balance.
42 *Proceedings of the National Academy of Sciences of the United States of America*,
43 100(17), 9892–9893. <https://doi.org/10.1073/pnas.1732012100>

- 1
2
3 1 Zevenbergen, L. W., & Thorne, C. R. (1987). Quantitative Analysis of Land Surface
4 2 Topography. *Earth Surface Processes and Landforms*, 12(1), 47–56.
- 6 3 Zhang, X., Friedl, M. A., Schaaf, C. B., Strahler, A. H., Hodges, J. C. F., Gao, F., ...
7 4 Huete, A. (2003). Monitoring Vegetation Phenology using MODIS. *Remote*
8 5 *Sensing of Environment*, 84(3), 471–475. <https://doi.org/10.1016/S0034->
9 6 [4257\(02\)00135-9](https://doi.org/10.1016/S0034-4257(02)00135-9)
- 11 7 Zhu, X., Chen, J., Gao, F., Chen, X., & Masek, J. G. (2010). An Enhanced Spatial and
12 8 Temporal Adaptive Reflectance Fusion Model for Complex Heterogeneous
13 9 Regions. *Remote Sensing of Environment*, 114(11), 2610–2623.
14 10 <https://doi.org/10.1016/j.rse.2010.05.032>

11

12